Eur. Phys. J. C 34, 345–360 (2004)
Digital Object Identifier (DOI) 10.1140/epjc/s2004-01726-4

THE EUROPEAN PHYSICAL JOURNAL C

Masses and couplings of vector mesons from the pion electromagnetic, weak, and $\pi\gamma$ transition form factors

D. Melikhov[1,a], O. Nachtmann[1,b], V. Nikonov[2,c], T. Paulus[1,d]

[1] Institut für Theoretische Physik, Philosophenweg 16, 69120 Heidelberg, Germany
[2] Petersburg Nuclear Physics Institute, Gatchina, 188300 St.-Petersburg, Russia

Received: 8 December 2003 /
Published online: 23 March 2004 –

Abstract. We analyze the pion electromagnetic, charged-current, and $\pi\gamma$ transition form factors at timelike momentum transfers q, $q^2 = s \leq 1.4\,\mathrm{GeV}^2$, using a dispersion approach. We discuss in detail the propagator matrix of the photon–vector meson system and define certain reduced amplitudes, or vertex functions, describing the coupling of this system to final states. We then apply the derived analytic expressions to the analysis of the recent $e^+e^- \to \pi^+\pi^-$, $\tau^- \to \pi^-\pi^0\nu_\tau$, and $e^+e^- \to \pi^0\gamma$ data. We find the reduced amplitudes for the coupling of the photon and vector mesons to two pseudoscalars to be constant, independent of s, in the range considered, indicating a "freezing" of the amplitudes for $s \leq 1\,\mathrm{GeV}$. The fit to the form factor data leads to the following values of the Breit–Wigner resonance masses $m_{\rho^-} = 775.3 \pm 0.8\,\mathrm{MeV}$, $m_{\rho^0} = 773.8 \pm 0.6\,\mathrm{MeV}$ and $m_\omega = 782.43 \pm 0.05\,\mathrm{MeV}$, where the errors are only statistical.

1 Introduction

The pion elastic and transition form factors at timelike momentum transfers provide an important source of information about the masses and coupling constants of the vector meson resonances ρ, ω, ϕ, etc. However, a reliable extraction of the resonance parameters from the experimental data is a complicated problem. The reason is that the direct QCD-based calculation of the form factors in terms of the resonance parameters is not possible yet, and hence one has to use approximate approaches. A typical procedure of extracting the vector meson parameters is as follows: One relies on some theoretical formula for the form factor in terms of the vector meson masses and couplings, and tries to extract their numerical values by fitting the experimental data. Most of the approaches providing theoretical inputs for the form factors in the region of vector meson resonances 0.7 to 1.2 GeV fall into the two big classes: approaches based on the vector meson dominance picture [1–6] and approaches based on the inclusion of vector mesons into the chiral perturbation theory framework [7–10].

No need to say that the extracted values of the meson parameters depend on the theoretical models used in this procedure; moreover, approximate formulas for the form factors in terms of the meson parameters inevitably introduce a systematic error which is extremely hard to control.

[a] e-mail: melikhov@thphys.uni-heidelberg.de
[b] e-mail: o.nachtmann@thphys.uni-heidelberg.de
[c] e-mail: nikonov@thd.pnpi.spb.ru
[d] Now at Philips; e-mail: timo.paulus@philips.com

Table 1. Values of the meson masses as quoted in the last three editions of PDG [11, 12]

	1998	2000	2002
ρ^0	770.0 ± 0.8	769.3 ± 0.8	771.1 ± 0.9
ω	781.94 ± 0.12	782.57 ± 0.12	782.57 ± 0.12

Neglecting systematic uncertainties may lead to controversies in the determination of the resonance parameters. To illustrate this statement, let us turn to Table 1 which presents the vector meson masses as quoted in the last three editions of the Particle Data Group [11,12]. One clearly sees a very small error and relatively sizable "time-variations" of the average values such that some of the results from different editions are only marginally compatible with each other within 3σ. Moreover, the value of the ρ-meson mass $m_\rho = 775.9 \pm 0.5\,\mathrm{MeV}$ as extracted from τ decays and e^+e^- annihilation data is well above the value of the ρ-meson mass as obtained by averaging all data [12].

The most natural explanation of this puzzle is that the systematic errors due to reliance on theoretical models may be underestimated. It is clear that a reliable extraction of the resonance parameters may only be reached if as broad as possible a set of data and reactions is used for the analysis. Comparison with the experiment serves as a test and to some extent a justification of the theoretical models and approximations employed.

The data on the $e^+e^- \to \pi^+\pi^-$, $\tau^- \to \pi^-\pi^0\nu_\tau$, and $e^+e^- \to \pi^0\gamma$ reactions offer a good possibility for extracting the ρ and ω masses and coupling constants and testing various theoretical models.

As a first step we discuss our dispersion-theoretical framework where we start from the photon γ and the vector meson V ($V = \rho, \omega, \ldots$) fields and identify the relevant amplitudes and couplings in a model-independent way. Then we introduce our model which takes into account only the most important contributions to the absorptive parts in the dispersion relations. In essence,
(i) we keep only the contributions of the $\pi\pi$ and KK intermediate states and
(ii) assume certain reduced amplitudes to be independent of the CM energy in the resonance region. Our approach does not use any specific effective Lagrangian or other approximation scheme, like the $1/N_c$ expansion. However, rigorous theoretical results which are known or may become available in the future, may be easily implemented in our framework as improved representations for the reduced amplitudes.

In the second step we apply our formalism to perform a simultaneous analysis of the pion electromagnetic, charged-current, and $\pi\gamma$ form factors. We obtain analytic expressions for the form factors in terms of the resonance parameters, paying special attention to the existing ambiguities in their definitions. We then apply our results to the F_π, F_π^+, and $F_{\gamma\pi}$ data and extract masses and couplings of the vector mesons. In this paper we consider only the most recent data [13–16] for these form factors in the range $2m_\pi \le \sqrt{s} \le 1.2\,\mathrm{GeV}$. We shall demonstrate that these data are well described by our model allowing for a reliable extraction of the vector meson parameters. A systematic analysis of all available form factor data using our model is left for future work. Then also relative normalization uncertainties between various data sets will have to be considered.

This paper is organized as follows: Sect. 2 gives definitions and summarizes important rigorous results for F_π and $F_{\gamma\pi}$. A general treatment of the vector meson–photon mixing in the framework of the dispersion approach is given in Sect. 3. Our model is formulated in Sect. 4. In Sect. 5 numerical results are presented. Conclusions are given in Sect. 6. Appendices contain the necessary technical details.

2 The pion electromagnetic, weak, and $\pi\gamma$ form factors

2.1 The electromagnetic form factor

The pion electromagnetic form factor is defined by

$$\langle\pi^+(p')|J_\mu(0)|\pi^+(p)\rangle = e(p'+p)_\mu F_\pi(q^2),\quad q = p' - p, \tag{1}$$

for $q^2 < 0$, and by

$$\langle\pi^+(p')\pi^-(p)|J_\mu(0)|0\rangle = e(p'-p)_\mu F_\pi(q^2),\quad q = p' + p, \tag{2}$$

for $q^2 > 0$. Here J_μ is the electromagnetic current and $e = \sqrt{4\pi\alpha_{\mathrm{e.m.}}}$. The form factor is normalized as $F_\pi(0) = 1$.

As a function of the complex variable $s = q^2$, the form factor $F_\pi(s)$ has a cut in the complex s-plane starting at the two-pion threshold $s = 4m_\pi^2$ which corresponds to two-pion intermediate states. There are also cuts related to $K\bar{K}$ intermediate states and multi-meson states (3π, etc.). The form factor in the timelike region ($s > 0$) is

$$F_\pi(s + \mathrm{i}\epsilon) = |F_\pi(s)|\mathrm{e}^{\mathrm{i}\delta_\pi(s)}, \tag{3}$$

where $\delta_\pi(s)$ is the phase. For the theoretical description of the form factor in different regions of momentum transfers, different theoretical approaches are used.

At large spacelike momentum transfers, $-q^2 \to \infty$, perturbative QCD (pQCD) gives rigorous predictions for the asymptotic behaviour of the form factor [17]

$$F_\pi(q^2) \sim \frac{8\pi f_\pi^2 \alpha_\mathrm{s}(-q^2)}{-q^2}, \tag{4}$$

where α_s is the QCD coupling parameter and $f_\pi = 130.7 \pm 0.4\,\mathrm{MeV}$ [12] is the pion decay constant defined by the relation

$$\langle 0|\bar{d}(0)\gamma_\mu\gamma_5 u(0)|\pi^+(p)\rangle = \mathrm{i}p_\mu f_\pi. \tag{5}$$

As the spacelike momentum transfer becomes smaller, the form factor turns out to be the result of the interplay of perturbative and non-perturbative QCD effects, with a strong evidence that non-perturbative QCD effects dominate in the region $0 \le -q^2 \le 10\,\mathrm{GeV}^2$ [18,19]. The picture based on the concept of constituent quarks which effectively account for non-perturbative dynamics has proven to be efficient for the description of the form factor in this region (see for instance [20]).

At large timelike momentum transfers, $s \ge 10$–$20\,\mathrm{GeV}^2$, $F_\pi(s)$ can be obtained from the analytic continuation of the pQCD formula (4). At small timelike momentum transfers the situation is more complicated since there dynamical details of the confinement mechanism are crucial. Quarks and gluons are no longer the degrees of freedom of QCD leading to a simple description of the form factor. At timelike momentum transfers we are essentially in the region of hadronic singularities and typically one relies on methods based on hadronic degrees of freedom. In the region of interest to us here, $q^2 = 0$–$1.5\,\mathrm{GeV}^2$, the lightest pseudoscalar mesons are most important. There are many approaches to understand the behaviour of the pion form factor at these timelike momentum transfers.

A popular approach is based on the vector meson dominance (VMD) model [1]. In the simplest version one considers just the contribution of the ρ-meson pole, which in combination with the normalization condition $F_\pi(s = 0) = 1$ leads to

$$F_\pi(s) = \frac{m_\rho^2}{m_\rho^2 - s}. \tag{6}$$

This simple formula works with a reasonable accuracy both for small spacelike momentum transfers and timelike momentum transfers below the $\pi\pi$ threshold: $-1\,\mathrm{GeV}^2 \le s \le 4m_\pi^2$. For s near the $\pi\pi$ threshold one should take into

account effects of the virtual pions. In this region, the momenta of the intermediate pions are small and a consistent description of the form factor is provided by chiral perturbation theory (ChPT) [7], the effective theory for QCD at low energies.

For higher s, in the region of ρ and ω resonances, a similar rigorous treatment of the form factor is still lacking, and one has to rely on model considerations. Gounaris and Sakurai (GS) [3] obtained the expression for the ρ-meson contribution to the pion form factor which takes into account the ρ-meson finite width due to the virtual pions. The GS form factor may be written in the form

$$F_\pi(s) = \frac{m_\rho^2 - B_{\rho\rho}^{\rm GS}(0)}{m_\rho^2 - s - B_{\rho\rho}^{\rm GS}(s)}. \tag{7}$$

The function $B_{\rho\rho}^{\rm GS}(s)$ corresponds to the two-pion loop diagram, but one can easily add the $K\bar{K}$ loop too; see Appendix B. The corresponding Feynman integral is linearly divergent, but its imaginary part is defined in a unique way. The real part may then be reconstructed by a doubly- subtracted dispersion representation. The Gounaris-Sakurai formula corresponds to the following prescription of fixing the subtraction constants

$$\mathrm{Re}\, B_{\rho\rho}^{\rm GS}(s)|_{s=m_\rho^2} = 0, \qquad \frac{\mathrm{d}}{\mathrm{d}s}\mathrm{Re}\, B_{\rho\rho}^{\rm GS}(s)|_{s=m_\rho^2} = 0. \tag{8}$$

The phase of the GS form factor

$$\tan\delta(s) = \frac{\mathrm{Im}B_{\rho\rho}^{\rm GS}(s)}{m_\rho^2 - s - \mathrm{Re}B_{\rho\rho}^{\rm GS}(s)} \tag{9}$$

agrees well with the experimental data in the region $4m_\pi^2 < s < 0.9\,\mathrm{GeV}^2$.

The Gounaris–Sakurai form factor (7) satisfies the relation $F_\pi(0) = 1$. But it turns out that it does not have enough flexibility to give at the same time a good description at the peak of the ρ resonance; see Appendix B.

Near the ρ-meson peak the ρ-meson contribution to the pion form factor can be expressed in terms of the $\gamma \to \rho \to \pi\pi$ matrix element as follows:

$$F_\pi(s) = \frac{\frac{1}{2} g_{\rho\to\pi\pi} f_\rho\, m_\rho}{m_\rho^2 - s - B_{\rho\rho}^{\rm GS}(s)}. \tag{10}$$

Here $g_{\rho\pi\pi}$ and f_ρ are defined according to

$$\langle \pi^+(p')\pi^-(p)|T|\rho(q,\varepsilon)\rangle = -\frac{1}{2} g_{\rho\to\pi\pi}\, \varepsilon_\mu \cdot (p'-p)^\mu, \tag{11}$$

$$\langle 0|J_\mu(0)|\rho^0(q,\varepsilon)\rangle = e f_\rho m_\rho \varepsilon_\mu, \tag{12}$$

where ε_μ is the ρ-meson polarization and q is the 4-momentum vector. Now $|F_\pi(s)|$ from (10) describes well the data for $s \simeq m_\rho^2$. But extrapolating (10) to $s = 0$ violates the normalization condition $F_\pi(0) = 1$ that is unacceptable.

Note that the definitions of $g_{\rho\to\pi\pi}$ and f_ρ in (12) are not really appropriate since they are based on ρ-meson states. But the ρ meson is a resonance and has no asymptotic states. Our precise definitions of $g_{\rho\to\pi\pi}$ and f_ρ will be given below in Sect. 4.

Thus, neither (7) nor (10) are suitable for the analysis of the form factor data for all $s = 0$–$1.5\,\mathrm{GeV}^2$. There were many attempts to modify the vector meson dominance or to use related approaches in order to bring the results on the pion form factor in agreement with the data (see [5,6,9] and the papers quoted therein). The pion form factor in the region $s = 0$–$1.5\,\mathrm{GeV}^2$ is one of the main sources for obtaining the masses and coupling constants of vector mesons. However, with different assumptions on the form of the vector-resonance contribution to the pion form factor one obtains different values of masses and couplings. Therefore a consistent description of the pion form factor in this region in terms of the low-lying mesons (π, K, ρ, ω) is crucial for extracting reliable values of these parameters. Interesting results have been obtained by the authors of [5] who noticed that an effective momentum-dependent $\rho\gamma$ coupling appears in the framework of the effective Lagrangian approach. This momentum-dependent $\rho\gamma$ coupling also improves the description of the pion form factor at small spacelike momentum transfers.

Clearly, to achieve a realistic description of the form factor, one has to account for vector meson finite-width and mixing effects. This may be done in a consistent way within a dispersion approach and will be the subject of Sect. 3.

2.2 The weak form factor

The $\pi^- \to \pi^0$ weak transition form factors parameterize the charged-current transition amplitude as follows:

$$\begin{aligned}&\langle \pi^+(p)\pi^0(p')|\bar{u}(0)\gamma_\mu d(0)|0\rangle \\ &\quad = \sqrt{2}F_\pi^+(q^2)(p'-p)_\mu + \sqrt{2}F_\pi^-(q^2)q_\mu.\end{aligned} \tag{13}$$

In the limit of the exact isospin symmetry we have $F_\pi^- = 0$ and $F_\pi^+ = F_\pi|_{\rm isovector}$. In practice we expect that the electromagnetic form factor F_π should be close to F_π^+ for $0 \le q^2 \le 1\,\mathrm{GeV}^2$ except for the region of the ω resonance. The form factor F_π contains an important isospin-violating contribution of the ω resonance, whereas there is no contribution analogous to ω in F_π^+.

2.3 The $\pi\gamma$ form factor

We shall be interested in the process $e^+e^- \to \gamma^* \to \pi^0\gamma$, where one of the photons is real and the other is virtual. The form factor $F_{\gamma\pi}$ relevant for this process is defined [19,21] according to

$$\begin{aligned}\langle \pi^0(p)\gamma(q',\varepsilon)|J_\mu(0)|0\rangle &= e^2\epsilon_{\alpha\beta\mu\nu}\varepsilon^{*\nu}q^\alpha q'^\beta F_{\gamma\pi}(q^2), \\ q &= p + q'.\end{aligned} \tag{14}$$

In terms of this form factor the $e^+e^- \to \pi^0\gamma$ cross section reads

$$\sigma_{e^+e^-\to\pi^0\gamma}(q^2) = \frac{2}{3}\pi^2\alpha_{\rm e.m.}^3 \left(1 - \frac{m_\pi^2}{q^2}\right)^3 |F_{\gamma\pi}(q^2)|^2. \tag{15}$$

In the chiral limit, $m_\pi^2 = 0$, the value of the form factor for $q^2 = 0$ is fixed by the Adler–Bell–Jackiw anomaly [22]:

$$F_{\gamma\pi}(0)|_{m_\pi^2=0} = \frac{1}{2\sqrt{2}\pi^2 f_\pi}. \tag{16}$$

In reality the pion is not massless, but still the anomaly provides a very good description of the observed $\pi^0 \to \gamma\gamma$ decay rate.

We shall therefore use the value (16) also for the physical pion in order to fix the form factor $F_{\gamma\pi}(0)$ in our analysis.

In the region of large spacelike momentum transfer q, the form factor can be calculated from pQCD with the result

$$F_{\gamma\pi}(q^2) \sim \frac{\sqrt{2}f_\pi}{-q^2}. \tag{17}$$

Brodsky and Lepage [23] proposed a simple formula,

$$F_{\gamma\pi}(q^2) = \frac{\sqrt{2}f_\pi}{4\pi^2 f_\pi^2 - q^2}, \tag{18}$$

which interpolates between $q^2 = 0$ and $q^2 \to -\infty$ and works well for all $q^2 < 0$. This formula may be written as

$$F_{\gamma\pi}(q^2) = \frac{\sqrt{2}f_\pi}{M_{\rm Res}^2 - q^2}, \tag{19}$$

with $M_{\rm Res} = 2\pi f_\pi = 880\,\mathrm{MeV}$, not too far from the masses of ρ and ω which give the dominant resonance contribution to the form factor.

To describe the form factor in the region $0 < q^2 \leq 1.5\,\mathrm{GeV}^2$, we should again use the meson degrees of freedom. For a realistic description of the form factors we must take into account finite-width and meson mixing effects.

3 Mixing of vector mesons: Propagator matrix and vertex functions

In this section we present model-independent considerations on the mixing of the photon with vector mesons.

Since vector mesons are unstable particles, one of the possibilities is to start with hypothetical stable states, which then get a width by inclusion of some interactions. This is an inherently perturbative picture which emerges for instance when the $1/N_c$ expansion is used.

We shall avoid such a perturbative approach and instead start with properly defined renormalized field operators with the quantum numbers of the vector mesons we are interested in. Clearly, such field operators can be defined in the framework of QCD. As the second step, we shall analyze the propagator matrix describing the mixing of these vector meson fields with the photon field. Then, we define certain transition amplitudes (or vertex functions) which are one-particle irreducible in the s channel, and establish the connection between these vertex functions and the experimentally measured form factors. These considerations are fully general and do not include any model assumptions. As the next step our model is formulated making certain assumptions for these vertex functions. This procedure is similar to the one used in [24] in the discussion of the γ–J/ψ mixing.

Let us consider the photon field $A_\mu(x)$ and a set of hermitian neutral vector meson fields $V_\mu^{(j)}(x)$ $(j = 2, \ldots, n)$. For convenience of notation we set $V_\mu^{(1)}(x) = A_\mu(x)$.

The fields $V_\mu^{(j)}(x)\,(j = 1, \ldots, n)$ have the same quantum numbers and therefore will have a $n \times n$ propagator matrix describing their mixing:

$$\Delta_{\mu\nu}^{(j,k)}(q) = \frac{1}{\mathrm{i}} \int \mathrm{d}^4x\, \mathrm{e}^{\mathrm{i}qx} \langle 0|T^*\{V_\mu^{(j)}(x)\, V_\nu^{(k)}(0)\}|0\rangle. \tag{20}$$

Here T^* is the covariant version of the T product; see for instance [25]. Using a covariant gauge for the photon, we can separate $\Delta_{\mu\nu}^{(j,k)}$ into transverse and longitudinal parts as follows:

$$\Delta_{\mu\nu}^{(j,k)} = \left(-g_{\mu\nu} + \frac{q_\mu q_\nu}{q^2 + \mathrm{i}\epsilon}\right) \Delta_{\rm T}^{(j,k)}(q^2) - \frac{q_\mu q_\nu}{q^2 + \mathrm{i}\epsilon}\, \Delta_{\rm L}^{(j,k)}(q^2). \tag{21}$$

The matrices

$$\Delta_{\rm T,L}(q^2) = \left(\Delta_{\rm T,L}^{(j,k)}(q^2)\right) \tag{22}$$

are analytic in the complex q^2-plane with cuts on the positive real axis. We shall always work to leading order in the electromagnetic interaction. Then the leftmost cut starts at $q^2 = 4m_\pi^2$, the two-pion threshold. Similarly, the transverse and the longitudinal structures can be isolated in the inverse propagator matrix

$$\left(\Delta^{-1}(q)\right)_{\mu\nu}^{(j,k)} = \left(-g_{\mu\nu} + \frac{q_\mu q_\nu}{q^2 + \mathrm{i}\epsilon}\right) \left(\Delta_{\rm T}^{-1}(q^2)\right)^{(j,k)} - \frac{q_\mu q_\nu}{q^2 + \mathrm{i}\epsilon}\, \left(\Delta_{\rm L}^{-1}(q^2)\right)^{(j,k)}. \tag{23}$$

The propagator matrix satisfies several general relations.
(1) Translation invariance of the vacuum gives

$$\Delta_{\mu\nu}^{(j,k)}(q) = \Delta_{\nu\mu}^{(k,j)}(-q). \tag{24}$$

(2) CPT-invariance gives

$$\Delta_{\mu\nu}^{(j,k)}(q) = \Delta_{\mu\nu}^{(j,k)}(-q). \tag{25}$$

(3) T-invariance of strong and electromagnetic interactions gives

$$\Delta_{\mu\nu}^{(j,k)}(q^0, \mathbf{q}) = \Delta^{(j,k)\mu\nu}(-q^0, \mathbf{q}). \tag{26}$$

From (24) we find that the matrices $\Delta_{\rm T,L}$ must be symmetric:

$$\left(\Delta_{\rm T,L}(q^2)\right)^{\rm T} = \Delta_{\rm T,L}(q^2), \tag{27}$$

whereas (25) and (26) are satisfied automatically and give no restrictions.

Using next the hermiticity of the fields $V_\mu^{(j)}(x)$ we get the unitarity relation for the propagator matrix

$$\begin{aligned}\Delta_{\mu\nu}^{(j,k)}(q) - \left(\Delta_{\nu\mu}^{(k,j)}(q)\right)^* &= \frac{1}{\mathrm{i}}\int \mathrm{d}^4x\, \mathrm{e}^{\mathrm{i}qx} \\ &\times\langle 0|\left\{V_\mu^{(j)}(x)V_\nu^{(k)}(0) + V_\nu^{(k)}(0)V_\mu^{(j)}(x)\right\}|0\rangle \\ = \frac{1}{\mathrm{i}}\sum_X \Big\{&(2\pi)^4\delta^{(4)}(q-p_X) \\ &\times\langle 0|V_\mu^{(j)}(0)|X(p_X)\rangle\langle X(p_X)|V_\nu^{(k)}(0)|0\rangle \\ +(2\pi)^4&\delta^{(4)}(q+p_X) \\ &\times\langle 0|V_\nu^{(k)}(0)|X(p_X)\rangle\langle X(p_X)|V_\mu^{(j)}(0)|0\rangle\Big\}.\end{aligned} \tag{28}$$

Here we have inserted a complete set of asymptotic (in strong interactions) states $|X(p_X)\rangle$, where p_X is the four-momentum. Note that the states $|X(p_X)\rangle$ contain pions and kaons, but no ρ or ω mesons, since the latter are unstable and thus have no asymptotic states.

Let us now define for all states $|X(p_X)\rangle$ the reduced, or amputated, matrix elements $\langle X(p_X)||V_\mu^{(j)}||0\rangle$ by taking out of $\langle X(p_X)|V_\mu^{(j)}|0\rangle$ all s channel V-propagator terms:

$$\langle X(p_X)|V_\mu^{(j)}|0\rangle = \langle X(p_X)|V^{(i)\nu}|0\rangle\left(\Delta^{-1}(p_X)\right)_{\nu\mu}^{(i,j)} \tag{29}$$

Here and in the following we use the summation convention. The inverse of (29) reads

$$\langle X(p_X)|V_\mu^{(j)}|0\rangle = \langle X(p_X)||V^{(i)\nu}||0\rangle\Delta_{\nu\mu}^{(i,j)}(p_X). \tag{30}$$

The reduced matrix elements, or vertex functions,

$$\langle X(p_X)||V_\mu^{(j)}||0\rangle$$

are one-V irreducible in the s channel.

It is convenient to define the transverse and the longitudinal components of the vertex functions

$$\begin{aligned}&\langle X(p_X)||V_{\mathrm{T}\mu}^{(j)}||0\rangle \\ &= \langle X(p_X)||V^{(j)\nu}||0\rangle\left(g_{\nu\mu} - \frac{(p_X)_\nu(p_X)_\mu}{(p_X)^2}\right), \\ &\langle X(p_X)||V_{\mathrm{L}}^{(j)}||0\rangle = \langle X(p_X)||V^{(j)\nu}||0\rangle\frac{(p_X)_\nu}{\sqrt{(p_X)^2}}.\end{aligned} \tag{31}$$

Now insert (30) into the unitarity relation (28). Considering first (28) for $q^0 > 0$, we obtain

$$\begin{aligned}&\Delta_{\mu\nu}^{(j,k)}(q) - \left(\Delta_{\nu\mu}^{(k,j)}(q)\right)^* = \\ &-\mathrm{i}\sum_X(2\pi)^4\delta^{(4)}(q-p_X)\left(\Delta_{\mu'\mu}^{(j',j)}\right)^*\langle X(p_X)||V^{(j')\mu'}||0\rangle^* \\ &\times\langle X(p_X)||V^{(k')\nu'}||0\rangle\Delta_{\nu'\nu}^{(k',k)}.\end{aligned} \tag{32}$$

Multiplying (32) by $\left(\Delta^{-1}\right)^\dagger$ from the left and by Δ^{-1} from the right we come to the unitarity relation for the inverse propagator (23):

$$\frac{1}{2i}\left\{\Delta_{\mathrm{T,L}}^{-1}(q^2) - \left(\Delta_{\mathrm{T,L}}^{-1}(q^2)\right)^\dagger\right\} = D_{\mathrm{T,L}}(q^2), \tag{33}$$

where the discontinuity matrices $D_{\mathrm{T,L}}(q^2)$ are given by

$$\begin{aligned}D_{\mathrm{T}}^{(j,k)}(q^2) = -\frac{1}{6}\sum_X&(2\pi)^4\delta^{(4)}(q-p_X) \\ &\times\langle X(p_X)||V_{T\lambda}^{(j)}||0\rangle^*\langle X(p_X)||V_T^{(k)\lambda}||0\rangle,\end{aligned} \tag{34}$$

$$\begin{aligned}D_{\mathrm{L}}^{(j,k)}(q^2) = -\frac{1}{2}\sum_X&(2\pi)^4\delta^{(4)}(q-p_X) \\ &\times\langle X(p_X)||V_L^{(j)}||0\rangle^*\langle X(p_X)||V_L^{(k)}||0\rangle.\end{aligned} \tag{35}$$

The discontinuity matrices satisfy the relations

$$\begin{aligned}&D_{\mathrm{T}}(q^2) = \left(D_{\mathrm{T}}(q^2)\right)^{\mathrm{T}} = \left(D_{\mathrm{T}}(q^2)\right)^\dagger, \\ &D_{\mathrm{T}}(q^2) = 0, \quad \text{for} \quad q^2 < 4m_\pi^2, \\ &D_{\mathrm{T}}(q^2) \geq 0, \quad \text{for} \quad q^2 \geq 4m_\pi^2,\end{aligned} \tag{36}$$

and

$$\begin{aligned}&D_{\mathrm{L}}(q^2) = \left(D_{\mathrm{L}}(q^2)\right)^{\mathrm{T}} = \left(D_{\mathrm{L}}(q^2)\right)^\dagger, \\ &D_{\mathrm{L}}(q^2) = 0, \quad \text{for} \quad q^2 < 4m_\pi^2, \\ &D_{\mathrm{L}}(q^2) \leq 0, \quad \text{for} \quad q^2 \geq 4m_\pi^2.\end{aligned} \tag{37}$$

Considering in (28) the case $q^0 < 0$, inserting (30) and using (24) we find exactly the same relations (33)– (37).

In our applications the longitudinal part $\Delta_{\mathrm{L}}(q^2)$ plays no role, so we concentrate on the transverse part $\Delta_{\mathrm{T}}(q^2)$ in the following.

The analytic properties of $\Delta_{\mathrm{T}}^{-1}(q^2)$ allow us to write a dispersion relation for it, which we assume to be convergent with two subtractions:

$$\Delta_{\mathrm{T}}^{-1}(q^2) = -M^2 + Kq^2 + (q^2)^2\frac{1}{\pi}\int\limits_{4m_\pi^2}^{\infty}\mathrm{d}s\frac{D_{\mathrm{T}}(s)}{s^2(s-q^2-\mathrm{i}\epsilon)}. \tag{38}$$

Here the subtraction terms M^2 and K have to be constant real symmetric matrices

$$M^2 = (M^2)^{\mathrm{T}} = (M^2)^*, \qquad K = K^{\mathrm{T}} = K^*. \tag{39}$$

This is as far as we can come with a general analysis of the propagator matrix.

In the next section we shall analyze the amplitude $\langle X(p_X)|A_\mu|0\rangle$ for the electromagnetic field and the state $|X(p_X)\rangle$ being the $\pi\pi$ state, which gives the pion form factor. Equation (30) with $j = 1$ represents this amplitude in terms of the vertex functions $\langle X(p_X)||V_\mu^{(i)}||0\rangle$ and the

propagator matrix $\Delta_{\mu\nu}$ for which we have the dispersion representation following from (38).

The merit of the representation (30) is that different types of singularities are isolated in different quantities: the propagator matrix contains the resonance poles which lead to "fast" variations of the form factors in the resonance region; the reduced amplitudes are free from these singularities and therefore represent slowly varying functions in the resonance region. To go further with the form factors we need some dynamical inputs for the vertex functions $\langle X(p_X)||V^{(j)\mu}||0\rangle$ and for the matrices M^2 and K; see Sect. 4.

Before going to the details of the model, note that we are free to change the basis for the fields. Defining new fields

$$\tilde{V}_\mu^{(j)}(x) = C_{jk}\, V_\mu^{(k)}(x), \tag{40}$$

with $C = (C_{jk})$ a real non-singular $n \times n$ matrix,[1] we get the propagator matrix of the new fields:

$$\tilde{\Delta}_{\mu\nu}(q) = C\Delta_{\mu\nu}(q)C^{\mathrm{T}}. \tag{41}$$

This leads to

$$\tilde{\Delta}^{-1}_{\mathrm{T,L}}(q^2) = \left(C^{-1}\right)^{\mathrm{T}} \Delta^{-1}_{\mathrm{T,L}}(q^2)C^{-1}, \tag{42}$$

$$\langle X(p_X)||\tilde{V}_\mu^{(j)}||0\rangle = \langle X(p_X)||V_\mu^{(k)}||0\rangle C^{-1}_{kj}. \tag{43}$$

The freedom of the field redefinition (40) can and will be used to impose certain constraints on the matrices M^2 and K in (38). If K is a positive-definite matrix – as it should, from the positivity of the metric for physical states in the Hilbert space – we can, for instance, diagonalize K and M^2 simultaneously by a transformation (40). The procedure to achieve this is completely analogous to the introduction of normal coordinates in the problem of small oscillations around a stable minimum of the potential in mechanics (see for instance [30]).

We should, however, be careful with redefinitions of the photon field $V_\mu^{(1)} = A_\mu$. A redefined photon field containing components proportional to the strong interaction vector fields $V_\mu^{(j)}$ with $j > 1$ will induce a direct quark–lepton coupling. We think this is unacceptable. The conditions which allow one to avoid this and to guarantee the massless photon and the correct charge normalization are summarized in Appendix A and lead to

$$M^2_{1j} = 0, \qquad j = 1, \ldots, n, \tag{44}$$

$$K_{11} = 1. \tag{45}$$

[1] In field theory we have also the freedom to make more complicated redefinitions of the fields, for instance

$$\tilde{V}_\mu(x) = (1 + c\,\partial^2)V_\mu(x), \quad c = \mathrm{const}.$$

Such transformations will change the q^2 behavior of the propagators and the p_X^2 behavior of the vertex functions. In the present article we will not explore further the possibility of such field redefinitions.

4 The γ–ρ–ω system

4.1 The model

We now apply the general considerations of the previous section to the system containing the photon field and the vector meson ρ and ω fields,

$$V_\mu^{(1)}(x) = A_\mu(x),$$
$$V_\mu^{(2)}(x) = \rho_\mu(x),$$
$$V_\mu^{(3)}(x) = \omega_\mu(x). \tag{46}$$

We suppose the field ρ_μ to be purely isovector, and ω_μ to be purely isoscalar. The electromagnetic coupling and isospin breaking from different up and down quark masses in QCD will introduce non-diagonal terms in the propagator matrix. In the following we will frequently use the indices γ, ρ, and ω instead of 1, 2, 3.

The 3×3 matrix M^2 of (38) and (39) for our system has to satisfy (44). By a linear transformation (40), but involving only the ρ and ω fields, we can make M^2 diagonal.

At this stage we define the ρ and ω mass squared parameters m_ρ^2 and m_ω^2 as zero points of the real parts of the diagonal terms of the inverse propagator matrix; that is, by the relations

$$\mathrm{Re}\left(\Delta^{-1}_{\mathrm{T}}\right)^{(\rho,\rho)}(m_\rho^2) = 0, \quad \mathrm{Re}\left(\Delta^{-1}_{\mathrm{T}}\right)^{(\omega,\omega)}(m_\omega^2) = 0. \tag{47}$$

Then we choose the normalization of the fields ρ_μ and ω_μ in such a way that the matrix M^2 has the form

$$M^2 = \begin{pmatrix} 0 & 0 & 0 \\ 0 & m_\rho^2 & 0 \\ 0 & 0 & m_\omega^2 \end{pmatrix}. \tag{48}$$

To calculate the dispersive part of the inverse propagator, we must restrict the set of the intermediate states $|X(p_X)\rangle$ to be included in the unitarity relation (32), and parameterize the reduced amplitudes of the fields $V_\mu^{(j)}$ between these states and the vacuum.

Assumption 1. As the intermediate states $|X(p_X)\rangle$ in the dispersion relation (38) with D_{T} given by (35) we shall consider only the $\pi^+\pi^-$, 3π, K^+K^-, and $K^0\bar{K}^0$ states.

For the $\pi^+\pi^-$ and KK states we have

$$\langle \pi^+(k_1)\pi^-(k_2)||V^{(j)}_{\mathrm{T}\mu}||0\rangle = g^{(j)}_{\pi\pi}(k_1 - k_2)_\mu,$$
$$\langle K^+(k_1)K^-(k_2)||V^{(j)}_{\mathrm{T}\mu}||0\rangle = g^{(j)}_{KK}(k_1 - k_2)_\mu, \tag{49}$$

where $g^{(j)}_{\pi\pi}$ and $g^{(j)}_{KK}$ are in general (slowly varying) functions of $(k_1 + k_2)^2$.

Assumption 2. In the region of interest we neglect the dependence of $g^{(j)}_{\pi\pi}$ and $g^{(j)}_{KK}$ on $(k_1 + k_2)^2$ and assume all $g^{(j)}$ to be real constants

$$g^{(1)}_{\pi\pi} = e, \quad g^{(2)}_{\pi\pi} = \frac{1}{2}g_{\rho\to\pi\pi}, \quad g^{(3)}_{\pi\pi} = \frac{1}{2}g_{\omega\to\pi\pi}, \tag{50}$$

and similarly for the KK intermediate states

$$g^{(1)}_{K^+K^-} = e, \qquad g^{(1)}_{K^0\bar{K}^0} = 0,$$
$$g^{(2)}_{K^+K^-} = -g^{(2)}_{K^0\bar{K}^0} = \frac{1}{2} g_{\rho\to KK},$$
$$g^{(3)}_{K^+K^-} = g^{(3)}_{K^0\bar{K}^0} = \frac{1}{2} g_{\omega\to KK}. \tag{51}$$

Here $g^{(1)}_{\pi\pi} = g^{(1)}_{K^+K^-} = e$ and $g^{(1)}_{K^0\bar{K}^0} = 0$ as required by the charge normalization of the π^+, K^+ and K^0; see Appendix C.

The decays $\rho \to K\bar{K}$ and $\omega \to K\bar{K}$ are forbidden kinematically at the ρ and ω peaks. This makes a direct determination of the corresponding coupling constants $g_{\rho\to KK}$ and $g_{\omega\to KK}$ difficult. Therefore we use as additional theoretical input the relations following from the approximate SU(3) flavor symmetry of strong interactions and ideal mixing of the vector mesons:

$$g_{\rho\to KK} = g_{\omega\to KK} = \frac{1}{2} g_{\rho\to\pi\pi}. \tag{52}$$

In this paper we do not analyze the 3π decays in detail. In the unitarity relation (32) and (33) the 3π intermediate states produce the width of the ω, Γ_ω, which is one of the fitting parameters.

We now have to specify the matrix K in (38). The explicit form of the matrix K is discussed in Appendix B, and here we present the final form for the inverse propagator matrix in our model:

$$\Delta^{-1}_{\mathrm{T}}(s) = \tag{53}$$
$$\begin{pmatrix} s & e\frac{f_\rho}{m_\rho}s + B_{\gamma\rho}(s) & e\frac{f_\omega}{m_\omega}s + B_{\gamma\omega}(s) \\ e\frac{f_\rho}{m_\rho}s + B_{\gamma\rho}(s) & -m_\rho^2 + s + B_{\rho\rho}(s) & s\,b_{\rho\omega} + B_{\rho\omega}(s) \\ e\frac{f_\omega}{m_\omega}s + B_{\gamma\omega}(s) & s\,b_{\rho\omega} + B_{\rho\omega}(s) & -m_\omega^2 + s + B_{\omega\omega}(s) \end{pmatrix}.$$

The functions B_{ij} are constructed by the doubly-subtracted dispersion integrals (38) corresponding to the pion and kaon contributions and include also the relevant subtraction terms defined such that

$$B_{ij}(s=0) = 0,$$
$$\mathrm{Re}B_{\rho\rho}(m_\rho^2) = \mathrm{Re}B_{\gamma\rho}(m_\rho^2) = \mathrm{Re}B_{\rho\omega}(m_\rho^2) = 0,$$
$$\mathrm{Re}B_{\omega\omega}(m_\omega^2) = \mathrm{Re}B_{\gamma\omega}(m_\omega^2) = 0. \tag{54}$$

For the functions B_{ij} defined according to the conditions (54), the dimensionful constants f_ρ and f_ω correspond to our precise definitions of the leptonic decay constants of the vector mesons. The detailed formulas for B_{ij} are given in Appendix B.

The intermediate $\pi\gamma$ states do not contribute to the form factors to first order in the e.m. coupling. Nevertheless, we need the reduced $\pi\gamma$ amplitudes for the description of the $\pi\gamma$ transition form factor. The reduced $\pi\gamma$ amplitudes have the form

$$\langle\pi(k_1)\gamma(k_2,\varepsilon)||V^{(j)}_\mu(0)||0\rangle = e\epsilon_{\alpha\beta\mu\nu}\varepsilon^{*\nu}k_1^\alpha k_2^\beta g^{(j)}_{\gamma\pi}, \tag{55}$$

where $g^{(j)}_{\gamma\pi}$ in general depend on $(k_1+k_2)^2$. We assume the $g^{(j)}_{\gamma\pi}$ to be constant as we did for the $\pi\pi$ and $K\bar{K}$ couplings. Then $g^{(1)}_{\gamma\pi}$ is determined from the anomaly (see Appendix C)

$$g^{(1)}_{\gamma\pi} = eF_{\gamma\pi}(0) = e\frac{1}{2\sqrt{2}\pi^2 f_\pi}. \tag{56}$$

The two additional dimensionless parameters $g_{\rho\to\gamma\pi} = m_\rho\, g^{(2)}_{\gamma\pi}$ and $g_{\omega\to\gamma\pi} = m_\omega\, g^{(3)}_{\gamma\pi}$ are assumed to be real.

Let us summarize the parameters of our model. These are

(1) the Breit–Wigner masses of the vector mesons, that is m_ρ and m_ω;
(2) the decay constants f_ρ, f_ω;
(3) the mixing parameter $b_{\rho\omega}$;
(4) the couplings of the vector mesons ρ and ω to two pions $g_{\rho\to\pi\pi}$, $g_{\omega\to\pi\pi}$;
(5) the width of the ω meson Γ_ω, and
(6) the $\pi\gamma$ couplings of the vector mesons $g_{\rho\to\pi\gamma}$ and $g_{\omega\to\pi\gamma}$.

Values for these parameters can be found by the fit to the available form factor data. However, it turned out that the parameters f_ω and Γ_ω cannot be well determined in this way from the reactions under discussion. The right place to extract these parameters from the experimental data is the reaction $e^+e^- \to \gamma^* \to 3\pi$, where the contribution of ω dominates. We leave a study of this reaction for a separate paper. Here we fix f_ω and Γ_ω to the PDG values, and leave only the remaining parameters from the list above free in the fits.

Clearly, the inclusion of higher resonances with the same quantum numbers in the mixing scheme is straightforward.

4.2 The form factors

The calculation of the form factors is now straightforward: we must reconstruct the propagator matrix from its inverse, and then calculate the amplitude $\langle X|A_\mu|0\rangle$ from (30) for the relevant final states. Finally we have to take into account that the amplitude of the e.m. current $\langle X(q)|J_\mu|0\rangle$ is related to the amplitude of the electromagnetic field as

$$\langle X(q)|J_\mu|0\rangle = \left(-g_{\mu\nu}q^2 + q_\mu q_\nu\right)\langle X(q)|A^\nu|0\rangle. \tag{57}$$

For the pion form factor the final state is the $\pi\pi$ state, and for the $\pi\gamma$ form factor it is the $\pi\gamma$ state. Since we work to first order in the e.m. coupling, the set of the intermediate states is the same in both cases. In the model described above it includes the $\pi\pi$, 3π, and KK intermediate states, and we use (49) and (55) for the vertex functions. To first order in the electromagnetic coupling the expressions for the pion elastic and the $\pi\gamma$ form factors obtained by the procedure described above may be written in a simple form (see Appendix C)

$$F_\pi(s) = 1 - sG^{\mathrm{T}}_{V\to\pi\pi}\tilde{\Delta}(s)G_{\gamma\to V}, \tag{58}$$
$$F_{\gamma\pi}(s) = F_{\gamma\pi}(0) - sG^{\mathrm{T}}_{V\to\pi\gamma}\tilde{\Delta}(s)G_{\gamma\to V}, \tag{59}$$

with $F_{\gamma\pi}(0)$ given by (56). The propagator matrix $\tilde{\Delta}$ here is the inverse of the vector meson block of the matrix $\Delta_{\rm T}^{-1}$, see (53):

$$\tilde{\Delta}^{-1} = \begin{pmatrix} -m_\rho^2 + s + B_{\rho\rho}(s) & s\, b_{\rho\omega} + B_{\rho\omega}(s) \\ s\, b_{\rho\omega} + B_{\rho\omega}(s) & -m_\omega^2 + s + B_{\omega\omega}(s) \end{pmatrix} \quad (60)$$

and

$$G_{V\to\pi\pi} = \begin{pmatrix} \frac{1}{2} g_{\rho\to\pi\pi} \\ \frac{1}{2} g_{\omega\to\pi\pi} \end{pmatrix},$$

$$G_{V\to\pi\gamma} = \begin{pmatrix} \frac{g_{\rho\to\pi\gamma}}{m_\rho} \\ \frac{g_{\omega\to\pi\gamma}}{m_\omega} \end{pmatrix},$$

$$G_{\gamma\to V} = \begin{pmatrix} \frac{f_\rho}{m_\rho} + \frac{B_{\gamma\rho}}{e\, s} \\ \frac{f_\omega}{m_\omega} + \frac{B_{\gamma\omega}}{e\, s} \end{pmatrix}. \quad (61)$$

In the case of the charged-current form factor F_π^+ (13) describing the $\pi^- \to \pi^0$ transition, the ω contribution is absent so we find from (134) of Appendix C

$$F_\pi^+(s) = \frac{m_\rho^2 - s + \frac{1}{2} g_{\rho\to\pi\pi} \frac{f_\rho s}{m_\rho}}{m_\rho^2 - s - B_{\rho\rho}(s)}. \quad (62)$$

Note that in the expressions for the pion electromagnetic and $\pi\gamma$ form factors (58) and (59), the parameters m_ρ and f_ρ are those of the ρ^0 meson, whereas in the formula for the charged-current form factor (62) the parameters refer to the ρ^- meson.

The expression (62) can be written in the "usual" vector meson dominance form (10)

$$F_\pi^+(s) = \frac{\frac{1}{2} g_{\rho\to\pi\pi} f_\rho^{\rm eff}(s) m_\rho}{m_\rho^2 - s - B_{\rho\rho}(s)}, \quad (63)$$

in terms of an effective s-dependent $\gamma\rho$ coupling

$$f_\rho^{\rm eff}(s) = f_\rho \frac{s}{m_\rho^2} + \frac{2(m_\rho^2 - s)}{g_{\rho\to\pi\pi} m_\rho}. \quad (64)$$

In this way we can make contact with the results of [5] where an s-dependent $\gamma\rho$ coupling is defined in an effective Lagrangian approach.

We use the expressions (58), (59) and (62) for the numerical analysis of the data for the pion electromagnetic, charged-current, and $\pi\gamma$ transition form factors in the next section.

5 Numerical results

We analyze the recent data on the pion electromagnetic form factor F_π (2), the charged-current form factor F_π^+ (13), and the $F_{\gamma\pi}$ form factor (14) in the region $\sqrt{s} = 0$–$1.2\,\text{GeV}$ using the formulae (58), (59), and (62), respectively. We take into account that the pion electromagnetic form factor F_π and the $\pi\gamma$ transition form factor $F_{\gamma\pi}$ contain contributions of the neutral ρ^0 and ω resonances, whereas the charged-current form factor F_π^+ contains the contribution of the ρ^- meson. Since we consider the isospin-violating ρ^0–ω mixing effects, we do not assume the parameters of the charged and the neutral ρ mesons to be equal to each other. We therefore fit the data for the F_π and $F_{\gamma\pi}$ form factors and extract in this way the ω and ρ^0 parameters. We use the recent SND data [16] for the form factor $F_{\gamma\pi}$ and the recent update [14] of the CMD-2 data [15] for F_π. We also include the available data on the phase of the electromagnetic form factor [27].

We separately fit the form factor F_π^+ and extract the ρ^- parameters from the CLEO data [13].

We perform different fitting procedures explained below. The fitted values of our parameters are given in Tables 2, 3 and 4.

Table 2. Parameters of the resonances as found by the fit to the form factors in the region $\sqrt{s} < 0.9\,\text{GeV}$ within the γ–ρ–ω mixing scheme (Fit I). Higher resonances are not included. The PDG value for f_ω is used. Fit to F_π and $F_{\gamma\pi}$: $\chi^2/\text{DOF} = 75/74$. Fit to the charged-current form factor F_π^+: $\chi^2/\text{DOF} = 11/23$. The $\rho\omega$ mixing parameter has the value $b_{\rho\omega} = (3.5 \pm 0.6)10^{-3}$

Res.	m_V, MeV	f_V, MeV	$g_{V\to\pi\gamma}$	$g_{V\to\pi\pi}$
ρ^-	775.5 ± 0.4	152.5 ± 0.33	–	11.52 ± 0.04
ρ^0	773.6 ± 0.5	154.1 ± 0.67	0.60 ± 0.06	11.43 ± 0.04
ω	782.42 ± 0.04	$\underline{45.3 \pm 0.9}$	1.79 ± 0.09	-0.27 ± 0.13

Table 3. Parameters of the resonances as found by the fit to the form factors in the region $\sqrt{s} < 0.9\,\text{GeV}$ (Fit II). The γ–ρ–ω mixing scheme with addition of the $\rho' = \rho(1450)$ is employed. The PDG values for f_ω and $m_{\rho'}$ are used. Fit to F_π and $F_{\gamma\pi}$: $\chi^2/\text{DOF} = 68/72$. Fit to F_π^+: $\chi^2/\text{DOF} = 11/21$. The parameters of ρ' cannot be determined by this fit. The $\rho\omega$ mixing parameter has the value $b_{\rho\omega} = (3.7 \pm 0.6)10^{-3}$

Res.	m_V, MeV	f_V, MeV	$g_{V\to\pi\gamma}$	$g_{V\to\pi\pi}$
ρ^-	775.3 ± 0.8	152.4 ± 0.4	–	11.50 ± 0.05
ρ^0	773.8 ± 0.6	155.3 ± 3.2	0.61 ± 0.06	11.53 ± 0.10
ω	782.43 ± 0.05	$\underline{45.3 \pm 0.9}$	1.76 ± 0.09	-0.31 ± 0.10
ρ'	$\underline{1465 \pm 25}$	–	–	–

Table 4. Fit to the data for $\sqrt{s} \le 1.2\,\text{GeV}$ (Fit III), where ρ, ω, $\rho' = \rho(1450)$, and $\rho'' = \rho(1700)$ are taken into account. Fit to F_π and $F_{\gamma\pi}$: $\chi^2/\text{DOF} = 72/89$. Fit to F_π^+: $\chi^2/\text{DOF} = 13/27$. The extracted ρ and ω couplings and masses are very stable with respect to inclusion/exclusion of ρ''. The couplings of ρ' and ρ'' correlate very strongly and cannot be reliably determined by this fit. The $\rho\omega$ mixing parameter has the value $b_{\rho\omega} = (3.5 \pm 0.5)10^{-3}$

Res.	m_V, MeV	f_V, MeV	$g_{V\to\pi\gamma}$	$g_{V\to\pi\pi}$
ρ^-	775.3 ± 0.5	151.5 ± 1.5	–	11.50 ± 0.05
ρ^0	773.7 ± 0.4	155.4 ± 1.7	0.65 ± 0.05	11.51 ± 0.07
ω	782.43 ± 0.05	$\underline{45.3 \pm 0.9}$	1.73 ± 0.08	-0.35 ± 0.10
ρ'	$\underline{1465 \pm 25}$	–	–	–
ρ''	$\underline{1700 \pm 20}$	–	–	–

The first fitting procedure (Fit I) includes the ρ^-, ρ^0, and ω contributions, and neglects the effects of higher resonances. We work in the region $\sqrt{s} \leq 0.9\,\text{GeV}$ where this approximation is checked to be self-consistent. The χ^2/DOF for this fit is 75/74 for F_π and $F_{\gamma\pi}$. It is 11/23 for F_π^+. The resulting values of the parameters are given in Table 2.

In the second step (Fit II), we study the stability of the extracted ρ and ω parameters with respect to the inclusion of higher resonances. This might serve as a probe of the systematic errors. We still stay in the region $\sqrt{s} \leq 0.9\,\text{GeV}$, but include in addition to ρ and ω also the $\rho' = \rho(1450)$ resonance. The contribution of the ρ' resonance to the form factors is obtained by adding the ρ' to the γ–ρ–ω mixing scheme (Appendix C) and neglecting the effects of mixing of ρ' with ρ and ω mesons. The ρ' mass is fixed according to PDG [12]. The parameters obtained by this procedure are given in Table 3. The quality of the fit to F_π and $F_{\gamma\pi}$ definitely improves (68/72), whereas for F_π^+ no improvement is seen. It is worth noting that the extracted parameters of the ρ and ω turn out to be very stable with respect to the inclusion/exclusion of ρ'.

In the third step, we extend our analysis to the region $\sqrt{s} \leq 1.2\,\text{GeV}$ (Fit III). We fit the form factors taking into account the three resonances ρ, ω, and ρ' (χ^2/DOF = 72/89 for F_π and $F_{\gamma\pi}$; χ^2/DOF = 13/27 for F_π^+). The results of this fit are given in Table 4. We then also include in addition the $\rho'' = \rho(1700)$. The coupling constants of ρ' and ρ'' turn out to be strongly correlated with each other and therefore cannot be extracted from the data under consideration. For a reliable extraction of these parameters one should go to higher values of s. Important for our analysis is that the masses and couplings of the ρ and ω mesons are remarkably stable with respect to inclusion/exclusion of ρ'' and very well compatible with the numbers obtained in Fits I and II. The form factors calculated with the parameters from Table 4 are shown in Figs. 1, 2, and 3 as solid lines.

The very satisfactory description of the data speaks in favor of the reliability of our assumptions of the dominance of the $\pi\pi$, KK, and 3π intermediate states and on the negligible s-dependence of the vertex functions.

Note that the masses of the charged and the neutral ρ mesons are different as obtained by our fits exposing an isospin violation in ρ mesons which is extensively discussed in the literature (see [31] and references therein).

However we would like to point out that assuming the parameters of the charged and the neutral ρ mesons to be equal to each other also leads to a very good description of the data with χ^2/DOF below 1 for all fitting procedures I-III (Fit I: χ^2/DOF = 94/100, Fit II: χ^2/DOF = 83/98, Fit III: χ^2/DOF = 86/121). Therefore, strictly speaking, the data analyzed by us here do not require the masses and couplings of the charged and neutral ρ mesons to be different. Still, we do not think it reasonable to take into account isospin-violating ρ–ω mixing effects and assume the absence of such effects in the charged and neutral ρ mesons. We therefore do not discuss in detail the fitting procedures in which the parameters of the charged and neutral mesons are assumed to be equal.

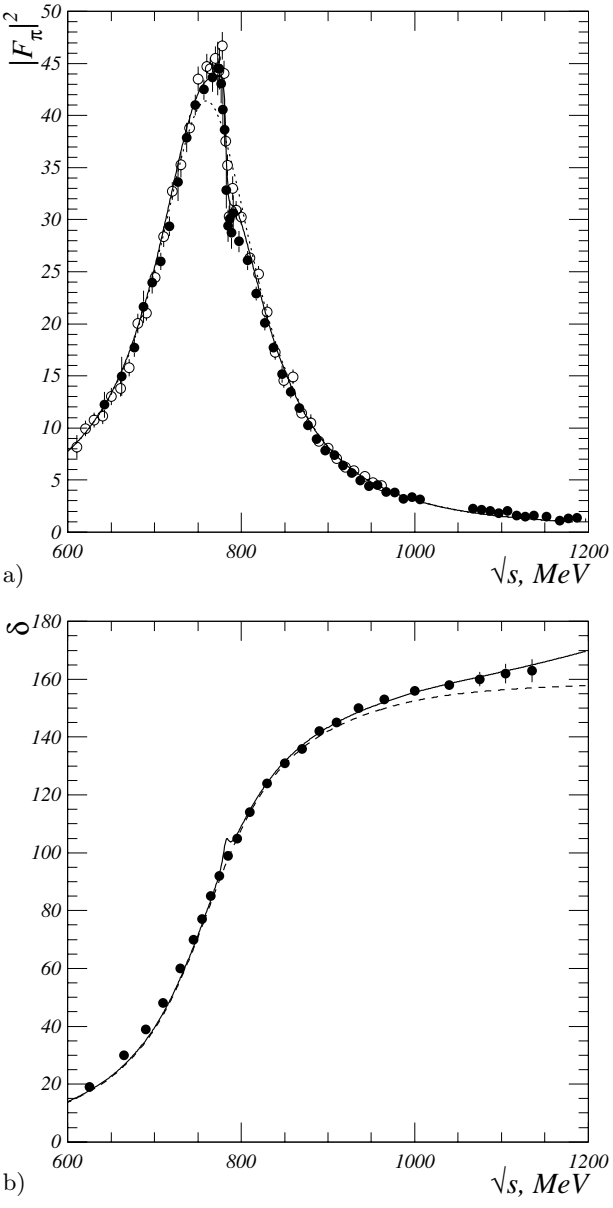

Fig. 1. The pion electromagnetic form factor $F_\pi(s)$: **a** Modulus squared: data from [14] (empty) used in the fit. Data from [26] (full) which were not used for the fit are shown for comparison. **b** Phase: data from [27]. Solid lines are for the full form factor as obtained by Fit III, dashed lines for the ρ contribution in (58)

Figure 4 shows the pion form factor at small spacelike momentum transfers, which was not included in the fit. Still one can see a good agreement with the data even down to $s = -2\,\text{GeV}^2$. The improvement of the description of F_π compared to the naive VMD Ansatz (6) shown as a dashed line is obvious. Similar results were obtained in [5].

Next we study the low energy expansion of the pion electromagnetic form factor near $s = 0$:

$$F_\pi(s) = 1 + \frac{1}{6}\langle r^2\rangle_V^\pi s + c_V^\pi s^2 + O(s^3). \qquad (65)$$

Here $\langle r^2\rangle_V^\pi$ is the squared charge radius of the pion. This quantity and c_V^π are of great interest in the framework of

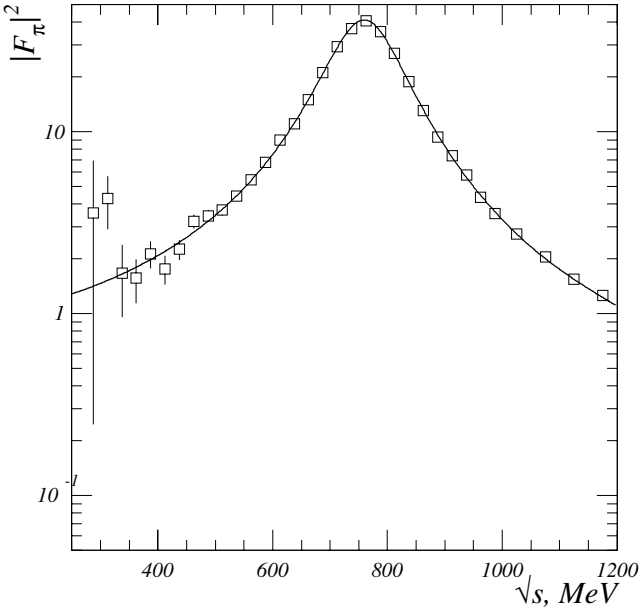

Fig. 2. The weak transition $\pi^- \to \pi^0$ form factor, Fit III. Data from [13]

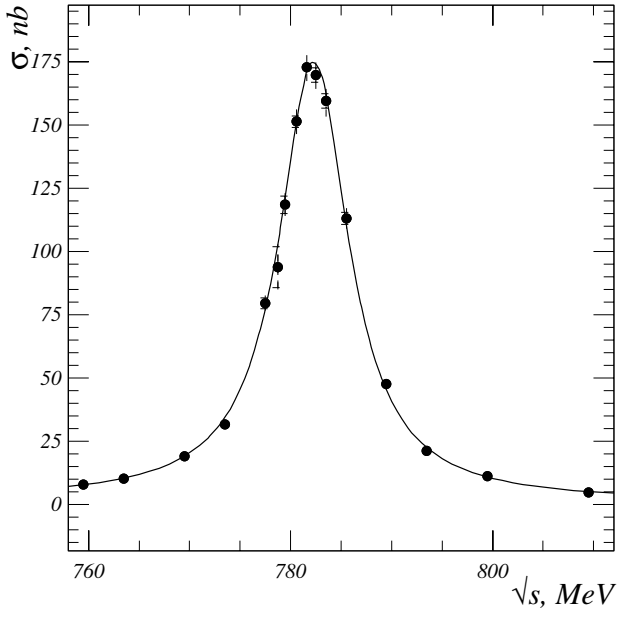

Fig. 3. The cross section $\sigma_{e^+e^-\to\pi\gamma}(Q^2)$, see (15), calculated with $F_{\gamma\pi}$ from (59). Data from [16]

ChPT for fixing certain parameters; see for instance [9,32]. In Table 5 we compare our results with those of [9,32] and the naive VMD. We find full consistency with ChPT within the errors which for our results are only statistical ones. Of course a study of systematic errors should also be done, but this is beyond the scope of this paper.

Finally, let us discuss the ρ and ω masses and the ρ width. The value of the ρ-meson Breit–Wigner mass defined according to (47), $m_{\rho^0} = 773.8 \pm 0.6\,\mathrm{MeV}$, agrees with the value obtained recently from the weak pion form factor [10],

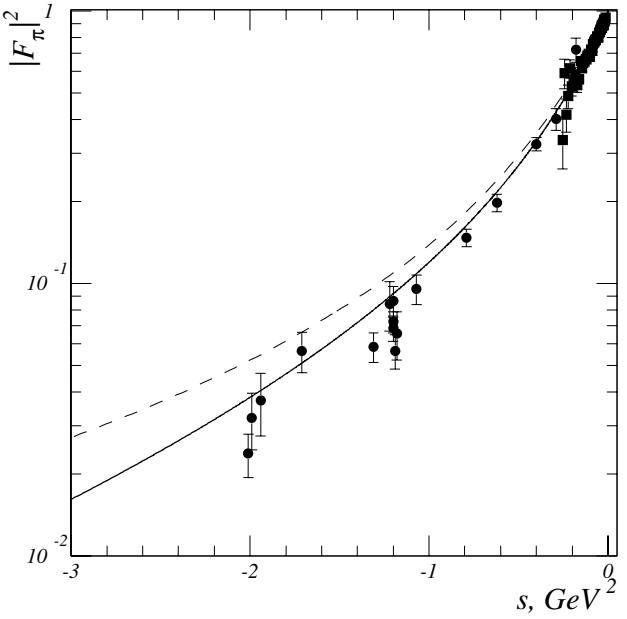

Fig. 4. The pion electromagnetic form factor $|F_\pi(s)|^2$ for $s < 0$. Data from [29]. Solid line: the full form factor from Fit III, dashed line: $F_\pi = 1/(1 - s/m_\rho^2)$

Table 5. The pion form factor at small momentum transfers. Coefficients of the expansion (65) from Fit III are given. The errors given in our results are only statistical emerging from errors in masses and couplings

	$\langle r^2\rangle_V^\pi$, GeV^{-2}	c_V^π, GeV^{-4}
Our result	11.41 ± 0.05	3.83 ± 0.02
ChPT to order $O(p^6)$ [32]	11.22 ± 0.41	3.85 ± 0.6
Results from [9]	11.04 ± 0.3	3.79 ± 0.04
Naive VMD (6)	10.16	2.8

and is sizably higher than the value $m_\rho = 771.1 \pm 0.9\,\mathrm{MeV}$ quoted by PDG.

The Breit–Wigner width of the ρ meson is defined according to the relation [10]

$$1/\Gamma_\rho^{\mathrm{BW}} = m_\rho \left.\frac{\mathrm{d}\delta_\pi(s)}{\mathrm{d}s}\right|_{s=m_\rho^2}, \tag{66}$$

where $\delta_\pi(s)$ is the phase of the pion form factor $F_\pi^+(s)$. Numerically, we obtain from Fit III for the charged ρ

$$\Gamma_\rho^{\mathrm{BW}} = 149.85 \pm 0.4\,\mathrm{MeV}.$$

Next we turn to the pole masses and widths of the ρ^-, ρ^0 and ω. For the charged ρ-meson the location of the pole in the second Riemann sheet of the s-plane is found by solving the equation

$$m_\rho^2 - s - B_{\rho\rho}(s) = 0. \tag{67}$$

The corresponding solution, s_{pole}, can be used in two different ways to define pole masses and pole widths. Either we choose to set

$$s_{\mathrm{pole}} = M'^2_\rho - \mathrm{i}\Gamma'^{\mathrm{pole}}_\rho M'_\rho, \tag{68}$$

Table 6. Pole masses and widths of ρ and ω

	ρ^+	ρ^0	ω
$M^{\rm pole}$, MeV	756.7 ± 0.4	755.0 ± 0.4	782.44 ± 0.05
$\Gamma^{\rm pole}$, MeV	144.7 ± 0.4	143.8 ± 0.4	8.38 ± 0.05

or

$$s_{\rm pole} = (M_\rho - {\rm i}\Gamma_\rho^{\rm pole}/2)^2. \tag{69}$$

The values obtained with the definition (69) are given in Table 6.

The pole masses of the ρ^0 and the ω meson are affected by the ρ–ω mixing effects and are obtained from (124):

$$\left\{m_\rho^2 - s - B_{\rho\rho}(s)\right\}\left\{m_\omega^2 - s - B_{\omega\omega}(s)\right\} - \left\{s\, b_{\rho\omega} + B_{\rho\omega}(s)\right\}^2 = 0. \tag{70}$$

The corresponding values of the pole masses and widths of the ρ^0 and ω are also given in Table 6.

6 Conclusions

We have discussed a general approach to the description of vector mesons and their mixing using dispersion relations. This approach allows us to represent various observables for the vector mesons as products of the vector meson propagator matrix and the reduced amplitudes (vertex functions). The unitarity relation gives the anti-hermitian part of the propagator matrix in terms of the relevant reduced amplitudes.

The merit of this approach lies in the possibility to separate different types of singularities in different quantities: the propagator matrix of the vector meson fields contains the resonance poles which lead to "fast" variations of the form factors in the resonance region, whereas the reduced amplitudes are free from these singularities and are therefore slowly varying functions in the resonance region. The description is fully general at this stage and contains no approximations. To go further we need some dynamical inputs for the reduced amplitudes.

We then formulate our model for the form factors based on the following assumptions:
(i) we take into consideration the resonances ρ, ω, and in a rough way also the $\rho(1450)$ and neglect higher vector mesons;
(ii) we take into account the $\pi\pi$, $K\bar{K}$ and effectively also the 3π intermediate states, and neglect contributions of multi-meson states in the unitarity relations;
(iii) we assume the scalar coupling factors in the reduced amplitudes to be constant in the region of the momentum transfer $\sqrt{s} = 0$–$1.2\,{\rm GeV}$.

On the basis of these assumptions we perform a combined analysis of the recent data for several reactions: $e^+e^- \to \pi^+\pi^-$, $\tau^- \to \pi^-\pi^0\nu_\tau$, and $e^+e^- \to \pi^0\gamma$ in the region of $\sqrt{s} = 0$–$1.2\,{\rm GeV}$. All the analyzed data is well described in our approach, allowing for an extraction of the resonance parameters, such as the Breit–Wigner masses and effective coupling constants. Our main numerical results are given in Tables 2–4.

These results are obtained by the fitting procedures, which allow for different masses and couplings of the charged and the neutral ρ mesons. Therefore, we have fitted separately the charged-current form factor F_π^+ and the neutral-current form factors F_π and $F_{\gamma\pi}$. Still we would like to point out that assuming the equality of the parameters of the charged and the neutral ρ mesons and fitting all three form factors F_π^+, F_π, and $F_{\gamma\pi}$ simultaneously also leads to a good description of the data with $\chi^2/{\rm DOF}$ below unity. However since the ρ–ω mixing and the isospin violation in ρ mesons are effects of the same nature, we do not think it reasonable to include only the first of these effects. We therefore do not discuss in detail the hypothesis that the masses and couplings of charged and neutral ρ mesons are equal.

The small errors of our results are statistical errors only indicating a good description of the data by our form factor formulae. Still our form factors are based on certain model assumptions; therefore a systematic error should be added.

One way to estimate the systematic error is to vary the fit range, to choose different parametrizations for the reduced amplitudes, and to study the corresponding variations of the fitted quantities. Partially, we did this by choosing various ranges of s and including higher resonances in our fits. We observed a good stability of the extracted resonance parameters and therefore do not expect the systematic error to be large. A more detailed study of the systematic errors is left for future work.

Further topics to be studied in the future are the inclusion of the ϕ meson in the mixing scheme and the implications of our form factor formulae for the theoretical values of the $g-2$ factor of the muon and the fine structure constant at the Z mass, $\alpha_{\rm s}(m_Z)$.

To summarize, we have obtained a very good description of the form factors in a model based on the unitarity and dispersion relations. Chiral perturbation theory constraints were checked to be respected. We have introduced reduced amlitudes or vertex functions which describe the coupling of the photon γ and of the vector meson ρ and ω fields to two pseudoscalar mesons and to $\pi\gamma$. These vertex functions contain invariant coupling functions which in principle depend on the momentum transfer $\sqrt{s}$. Perhaps the most interesting result of our study is that these invariant coupling functions are really coupling *constants* for $0 \le \sqrt{s} \le 1.0\,{\rm GeV}$. Thus these couplings are "frozen" below the GeV scale. This may perhaps be related to the expectation mentioned frequently in the literature [33] that in QCD the coupling parameter $\alpha_{\rm s}(\mu^2)$ is "frozen" for $\mu^2 \le 1\,{\rm GeV}^2$.

Acknowledgements. We are grateful to V.V. Anisovich, N. Brambilla, E. De Rafael, A. Donnachie, C. Ewerz, M. Jamin, F. Nagel, and B. Stech for useful discussions and to J. Urheim for correspondence on the CLEO data. We also thank M. Jamin for a careful reading of the manuscript. This work was supported by the Alexander von Humboldt-Stiftung and Bundesministerium für Bildung und Forschung project 05 HT 1VHA/0.

Appendix

A Gauge invariance and properties of the matrices M^2 and K

Here we study the conditions to be imposed on the propagator matrix (20) arising from the requirements to have a massless photon, the correct charge normalization, and no strong-interaction long-range force. This leads to the following constraints at $q^2 \to 0$:

$$\Delta_{\rm T}^{(1,1)}(q^2) = \frac{1}{q^2}\left(1 + O(q^2)\right), \tag{71}$$

$$\Delta_{\rm T}^{(i,j)}(q^2) = O(1), \quad \text{for } (i,j) \neq (1,1). \tag{72}$$

These conditions require the matrices M^2 and K to satisfy

$$M_{1j}^2 = 0, \quad \text{for } j = 1,\dots,n, \tag{73}$$

$$K_{11} = 1. \tag{74}$$

To show this, we note first that by a transformation of the type (40), but involving only $V_\mu^{(j)}$ with $j > 1$, we can always achieve

$$M_{1j}^2 = 0, \quad \text{for } j > 2. \tag{75}$$

Then the matrix M^2 takes the form

$$M^2 = \left(\begin{array}{c|cccc} M_{11}^2 & M_{12}^2 & 0 & \dots & 0 \\ \hline M_{12}^2 & & & & \\ 0 & & & & \\ . & & & M^{2'} & \\ 0 & & & & \end{array}\right), \tag{76}$$

where

$$M^{2'} = \begin{pmatrix} M_{22}^2 & \dots & M_{2n}^2 \\ . & \dots & . \\ M_{n2}^2 & \dots & M_{nn}^2 \end{pmatrix}. \tag{77}$$

For $n > 2$ we define

$$M^{2''} = \begin{pmatrix} M_{33}^2 & \dots & M_{3n}^2 \\ . & \dots & . \\ M_{n3}^2 & \dots & M_{nn}^2 \end{pmatrix}, \tag{78}$$

and for $n = 2$ we set $M^{2''} = 1$.

In the following we assume that $M^{2'}$ is a positive-definite matrix. This means, for instance, that all fields $V_\mu^{(j)}$, $j = 2,\dots,n$ must be independent.

From (38) and (76) we find now for $q^2 \to 0$

$$\begin{aligned} \det \Delta_{\rm T}^{-1}(q^2) &= (-1)^n \det M^2 + O(q^2) \\ &= (-1)^n \left[M_{11}^2 \det M^{2'} - \left(M_{12}^2\right)^2 \det M^{2''}\right] + O(q^2), \end{aligned} \tag{79}$$

$$\begin{aligned} \Delta_{\rm T}^{(1,1)}(q^2) &= \frac{\det\left(-M^{2'}\right) + O(q^2)}{\det \Delta_{\rm T}^{-1}(q^2)} \\ &= \frac{-\det M^{2'} + O(q^2)}{\det M^2 + O(q^2)}, \end{aligned} \tag{80}$$

$$\begin{aligned} \Delta_{\rm T}^{(1,2)}(q^2) &= \frac{(-1)^n M_{12}^2 \det M^{2''} + O(q^2)}{\det \Delta_{\rm T}^{-1}(q^2)} \\ &= \frac{M_{12}^2 \det M^{2''} + O(q^2)}{\det M^2 + O(q^2)}. \end{aligned} \tag{81}$$

We see now from (80) that in order to fulfill (72) we must have $\det M^2 = 0$. Then (72) for $(i,j) = (1,2)$ and (81) require $M_{12}^2 = 0$. Combining this result with (79) gives $M_{11}^2 = 0$. Recall that we assumed $M^{2'} > 0$ which implies also $M^{2''} > 0$. Thus, we have already demonstrated (73). Inserting now (73) into (38) gives

$$\det \Delta_{\rm T}^{-1}(q^2) = (-1)^{n-1} q^2 K_{11} \det M^{2'} + O\left((q^2)^2\right). \tag{82}$$

With (80) this leads to

$$\begin{aligned} \Delta_{\rm T}^{(1,1)}(q^2) &= \frac{(-1)^{n-1}\det M^{2'} + O(q^2)}{(-1)^{n-1} q^2 K_{11} \det M^{2'} + O\left((q^2)^2\right)} \\ &= \frac{1}{q^2 K_{11}}\left(1 + O(q^2)\right). \end{aligned} \tag{83}$$

To fulfill (72) we must, therefore, have $K_{11} = 1$ which proves (74).

B The inverse propagator matrix for the γ–ρ–ω system

Given (48), the inverse propagator (38) for the γ–ρ–ω system can be written as

$$\begin{aligned} \Delta_{\rm T}^{-1}(s) = &- \begin{pmatrix} 0 & 0 & 0 \\ 0 & m_\rho^2 & 0 \\ 0 & 0 & m_\omega^2 \end{pmatrix} + sK \\ &+ s^2 \frac{1}{\pi} \int\limits_{4m_\pi^2}^{\infty} {\rm d}s' \frac{D_{\rm T}(s')}{s'^2(s' - s - {\rm i}\epsilon)}. \end{aligned} \tag{84}$$

Here we set $q^2 = s$ and $D_{\rm T}(s')$ is obtained using Assumptions 1 and 2 of Sect. 4 and (35).

It is convenient to split the constant matrix K into two parts

$$K = K^a + K^b, \tag{85}$$

to be specified later, and to define the matrix function

$$B(s) = sK^a + s^2 \frac{1}{\pi} \int\limits_{4m_\pi^2}^{\infty} {\rm d}s' \frac{D_{\rm T}(s')}{s'^2(s' - s - {\rm i}\epsilon)}. \tag{86}$$

We thus have

$$\frac{1}{2{\rm i}}\left\{B(s) - B^\dagger(s)\right\} = D_{\rm T}(s). \tag{87}$$

The matrix K^a will be chosen such that it cancels the real part of the dispersive contribution to $B(s)$ in (86) at some specific values of s. Then splitting the matrix K according to (85) has an unambiguous physical meaning.

We choose $K^a_{\gamma\gamma} = 0$. With this, the condition (45) requires $K^b_{\gamma\gamma} = 1$.

The diagonal elements K^a_{VV}, $V = \rho, \omega$, are chosen such that they cancel the real part of the dispersive contribution in (86) at $s = m_V^2$ for the vector meson V. That is, we require

$$\mathrm{Re}\, B_{\rho\rho}(m_\rho^2) = 0, \qquad \mathrm{Re}\, B_{\omega\omega}(m_\omega^2) = 0. \tag{88}$$

The normalizations for the ρ and ω fields are fixed by requiring (48). Given (88), this requirement leads to

$$K^b_{\rho\rho} = K^b_{\omega\omega} = 1. \tag{89}$$

The non-diagonal matrix elements $(K^a)_{\gamma V}$ are chosen to cancel the real part of the dispersive contribution to $B_{\gamma V}$ at the point $s = m_V^2$. That is, we require

$$\mathrm{Re}\, B_{\gamma\rho}(m_\rho^2) = 0, \qquad \mathrm{Re}\, B_{\gamma\omega}(m_\omega^2) = 0. \tag{90}$$

Now we set

$$(K^b)_{\gamma V} = e\frac{f_V}{m_V}, \tag{91}$$

where the real parameters f_V correspond to our precise definitions of the leptonic decay constants of the vector mesons $V = \rho, \omega$.

Finally, the matrix element $(K^a)_{\rho\omega}$ is chosen such that it cancels the real part of the dispersive contribution to $B_{\rho\omega}$ in (86) at the point $s = m_\rho^2$. Thus we require

$$\mathrm{Re}\, B_{\rho\omega}(m_\rho^2) = 0. \tag{92}$$

Then the element

$$(K^b)_{\rho\omega} = b_{\rho\omega} \tag{93}$$

defines our $\rho-\omega$ mixing parameter. Clearly the value of the mixing parameter depends on the choice of the subtraction point in (92), but the physics, of course, does not.

Let us now discuss in more detail each of the functions $B_{ij}(s)$ of (86).

B.1 $B_{\rho\rho}$

The function $\mathrm{Im}\, B_{\rho\rho}$ receives contributions from the $\pi^+\pi^-$, K^+K^- and $K^0\bar{K}^0$ intermediate states. The two-pion contribution to $\mathrm{Im}\, B_{\rho\rho}$ reads

$$\mathrm{Im}\, B_{\rho\rho}(s)|_{\pi\pi} = g^2_{\rho\to\pi\pi}\mathrm{Im}\, B_{\pi\pi}(s), \tag{94}$$

where

$$\mathrm{Im}\, B_{\pi\pi}(s) = I(s, m_\pi^2),$$

$$I(s, m^2) = \frac{1}{192\pi}s\left(1 - \frac{4m^2}{s}\right)^{3/2}\theta(s - 4m^2). \tag{95}$$

We have to take into account also the K^+K^- and $K^0\bar{K}^0$ intermediate states which give contributions similar to (94) and (95) with π replaced by K. The coupling constant $g_{\rho\to KK}$ cannot be measured directly so we use the flavor-SU(3) relations (52)

$$2g_{\rho\to KK} = g_{\rho\to\pi\pi}. \tag{96}$$

Then we find

$$\begin{aligned}&\mathrm{Im}\, B_{\rho\rho}(s)\\ &= g^2_{\rho\to\pi\pi}\left[\mathrm{Im}\, B_{\pi\pi} + \frac{1}{4}\left(\mathrm{Im}\, B_{K^+K^-} + \mathrm{Im}\, B_{K^0\bar{K}^0}\right)\right]\\ &= g^2_{\rho\to\pi\pi}\left[\mathrm{Im}\, B_{\pi\pi} + \frac{1}{2}\mathrm{Im}\, B_{KK}\right].\end{aligned} \tag{97}$$

As explained above, see (88), we require

$$\mathrm{Re}\, B_{\rho\rho}(m_\rho^2) = 0. \tag{98}$$

Putting everything together we find from (86)

$$\begin{aligned}&B_{\rho\rho}(s) = g^2_{\rho\to\pi\pi}\, s\\ &\times\left[R(s, m_\pi^2) - R(m_\rho^2, m_\pi^2) + \frac{R(s, m_K^2) - R(m_\rho^2, m_K^2)}{2}\right]\\ &+ \mathrm{i}g^2_{\rho\to\pi\pi}\left[I(s, m_\pi^2) + \frac{I(s, m_K^2)}{2}\right].\end{aligned} \tag{99}$$

Here $I(s, m^2)$ is defined in (95), and

$$\begin{aligned}R(s, m^2) &= \frac{s}{192\pi^2}\ \mathrm{V.P.}\int_{4m^2}^{\infty}\frac{\mathrm{d}s'}{(s'-s)s'}\left(1 - \frac{4m^2}{s'}\right)^{3/2}\\ &= \begin{cases}\frac{1}{96\pi^2}\left(\frac{1}{3} + \xi^2 + \frac{\xi^3}{2}\log\left(\frac{1-\xi}{1+\xi}\right)\right), & \xi = \sqrt{1 - \frac{4m^2}{s}},\\ & \text{for } s > 4m^2,\\ \frac{1}{96\pi^2}\left(\frac{1}{3} - \xi^2 + \xi^3\arctan\left(\frac{1}{\xi}\right)\right), & \xi = \sqrt{\frac{4m^2}{s} - 1},\\ & \text{for } 0 < s < 4m^2,\\ \frac{1}{96\pi^2}\left(\frac{1}{3} + \xi^2 + \frac{\xi^3}{2}\log\left(\frac{\xi-1}{\xi+1}\right)\right), & \xi = \sqrt{1 - \frac{4m^2}{s}},\\ & \text{for } s < 0,\end{cases}\end{aligned} \tag{100}$$

where V.P. means the principle value.

B.2 $B_{\omega\omega}$

When considering the $B_{\omega\omega}$, the contributions of the intermediate K^+K^-, $K^0\bar{K}^0$, and 3π states should be taken into account.

First, recall that the coupling constant $g_{\omega\to 3\pi}$ is much smaller than the coupling constant $g_{\omega\to KK}$. This becomes

clear by using the SU(3) relation $g_{\omega\to KK}=\frac{1}{2}g_{\rho\to\pi\pi}$. Therefore, the contribution of the 3π intermediate states can be safely neglected in the real part of $B_{\omega\omega}$.

However, the decay $\omega\to K\bar{K}$ is forbidden kinematically. Due to this, the ω width emerges mainly due to the 3π intermediate states and is small because $g_{\omega\to 3\pi}$ is small. Therefore, the 3π states are crucial for the calculation of the imaginary part of $B_{\omega\omega}$ below the $K\bar{K}$ threshold. Still, the s-dependence of Im $B_{\omega\omega}$ can in practice be neglected, and we may therefore use for it a constant width approximation: $\Gamma_\omega=$ const. Taking into account that $B_{\omega\omega}=0$ for $s=0$, see (54), and making use of (88), we can write with sufficient accuracy for our purposes

$$B_{\omega\omega}(s)=g^2_{\omega\to KK}\;s\left[R(s,m_K^2)-R(m_\omega^2,m_K^2)\right] +\mathrm{i}\Gamma_\omega s/m_\omega. \tag{101}$$

B.3 $B_{\gamma\rho}$

The function Im $B_{\gamma\rho}$ receives contributions from the $\pi^+\pi^-$ and K^+K^- intermediate states. Taking into account the SU(3) relations (52) between the coupling constants we find

$$\begin{aligned}\text{Im }B_{\gamma\rho}&=2\,e\,g_{\rho\to\pi\pi}\left(\text{Im }B_{\pi\pi}+\frac{1}{2}\text{Im }B_{K^+K^-}\right)\\&=2\,e\,g_{\rho\to\pi\pi}\left(\text{Im }B_{\pi\pi}+\frac{1}{2}\text{Im }B_{KK}\right),\end{aligned} \tag{102}$$

and hence from (99)

$$\text{Im }B_{\gamma\rho}(s)=\frac{2\,e}{g_{\rho\to\pi\pi}}\,\text{Im }B_{\rho\rho}(s). \tag{103}$$

With the conditions (88) and (90) we get also

$$B_{\gamma\rho}(s)=\frac{2\,e}{g_{\rho\to\pi\pi}}B_{\rho\rho}(s). \tag{104}$$

B.4 $B_{\gamma\omega}$

The function Im $B_{\gamma\omega}$ receives contributions from the K^+K^- intermediate states:

$$\text{Im }B_{\gamma\omega}=2eg_{\omega\to KK}\text{Im }B_{K^+K^-}. \tag{105}$$

Requiring (90) we come to the expression

$$B_{\gamma\omega}(s)=2eg_{\omega\to KK}\;s\left[R(s,m_K^2)-R(m_\omega^2,m_K^2)\right] +2\mathrm{i}eg_{\omega\to KK}\;I(s,m_K^2). \tag{106}$$

B.5 $B_{\rho\omega}$

The imaginary part of $B_{\rho\omega}$ is given by the $\pi\pi$ intermediate states, so we have

$$\text{Im }B_{\rho\omega}(s)=g_{\rho\to\pi\pi}g_{\omega\to\pi\pi}\text{Im }B_{\pi\pi}(s). \tag{107}$$

Making use of (92), $B_{\rho\omega}$ takes the form

$$B_{\rho\omega}(s)=g_{\rho\to\pi\pi}g_{\omega\to\pi\pi} \times\left[s\,R(s,m_\pi^2)-s\,R(m_\rho^2,m_\pi^2)+\mathrm{i}I(s,m_\pi^2)\right]. \tag{108}$$

This completes our discussion of the individual functions $B_{ij}(s)$. The resulting inverse propagator matrix is given in (53). For comparison with (38) we also list the resulting matrix elements of K

$$\begin{aligned}K_{\gamma\gamma}&=1,\\K_{\rho\rho}&=1-g^2_{\rho\to\pi\pi}\left[R(m_\rho^2,m_\pi^2)+\frac{1}{2}R(m_\rho^2,m_K^2)\right],\\K_{\omega\omega}&=1-g^2_{\omega\to KK}R(m_\omega^2,m_K^2),\\K_{\gamma\rho}&=K_{\rho\gamma}\\&=e\frac{f_\rho}{m_\rho}-2eg_{\rho\to\pi\pi}\left[R(m_\rho^2,m_\pi^2)+\frac{1}{2}R(m_\rho^2,m_K^2)\right],\\K_{\gamma\omega}&=K_{\omega\gamma}=e\frac{f_\omega}{m_\omega}-2eg_{\omega\to KK}R(m_\omega^2,m_K^2),\\K_{\rho\omega}&=K_{\omega\rho}=b_{\rho\omega}-g_{\omega\to\pi\pi}g_{\rho\to\pi\pi}R(m_\rho^2,m_\pi^2),\end{aligned} \tag{109}$$

with the functions R given in (100).

Using the values for the masses and coupling constants from Fit III, we find the following central values for K_{ij}: $K_{\rho\rho}=1.017$, $K_{\omega\omega}=0.994$, $K_{\rho\omega}=2.6\cdot10^{-3}$, $K_{\gamma\rho}=0.2\,e$, $K_{\gamma\omega}=0.06\,e$, $e=\sqrt{4\pi\alpha_{\text{e.m.}}}\simeq 1/3$. Clearly, the deviation of the matrix K from the 3×3 unit matrix is small: only at the percent level.

Finally, we discuss the relation of our expressions to the original Gounaris–Sakurai expression for the form factor. The formula given in (11) of [3] can be written as

$$F_\pi^{\text{GS}}(s)=\frac{m_\rho^2+d\,m_\rho\Gamma_\rho^{\text{GS}}}{m_\rho^2-s-B_{\rho\rho}^{\text{GS}}(s)}, \tag{110}$$

where

$$\begin{aligned}B_{\rho\rho}^{\text{GS}}(s)&=-\Gamma_\rho^{\text{GS}}\left(\frac{m_\rho^2}{k_\rho^3}\right)\\&\quad\times\left\{k^2[h(s)-h(m_\rho^2)]+k_\rho^2h'(m_\rho^2)(m_\rho^2-s)\right\}\\&\quad+\mathrm{i}m_\rho\Gamma_\rho^{\text{GS}}\,(k/k_\rho)^3\,m_\rho/\sqrt{s},\end{aligned} \tag{111}$$

$$k=\begin{cases}\left(\frac{1}{4}s-m_\pi^2\right)^{1/2} & \text{for}\quad s\geq4m_\pi^2,\\ \mathrm{i}\left(m_\pi^2-\frac{1}{4}s\right)^{1/2} & \text{for}\quad 0\leq s<4m_\pi^2,\end{cases} \tag{112}$$

$$d=\frac{3}{\pi}\frac{m_\pi^2}{k_\rho^2}\log\left(\frac{m_\rho+2k_\rho}{2m_\pi}\right)+\frac{m_\rho}{2\pi k_\rho}-\frac{m_\pi^2m_\rho}{\pi k_\rho^3}, \tag{113}$$

$$h(s)=\frac{2}{\pi}\frac{k}{\sqrt{s}}\log\left(\frac{\sqrt{s}+2k}{2m_\pi}\right). \tag{114}$$

The only free parameters in the GS formula are m_ρ and Γ_ρ^{GS}. It is easy to see that the following relations hold:

$$\text{Re}\,B_{\rho\rho}^{\text{GS}}(m_\rho^2)=0,$$

$$\frac{\mathrm{d}}{\mathrm{d}s}\mathrm{Re}\,B^{\rm GS}_{\rho\rho}(s)|_{s=m_\rho^2}=0,$$
$$B^{\rm GS}_{\rho\rho}(0)=-d\,m_\rho\,\Gamma^{\rm GS}_\rho. \qquad (115)$$

This proves (7) and (8). Comparing (111) to (95) and (100) and setting

$$\Gamma^{\rm GS}_\rho=g^2_{\rho\to\pi\pi}\frac{1}{24\pi}\frac{k^3_\rho}{m^2_\rho}\left(1-\frac{B^{\rm GS}_{\rho\rho}(0)}{m^2_\rho}\right), \qquad (116)$$

we obtain

$$B^{\rm GS}_{\rho\rho}(s)=\left(1-\frac{B^{\rm GS}_{\rho\rho}(0)}{m^2_\rho}\right)\tilde B_{\rho\rho}(s)-\frac{B^{\rm GS}_{\rho\rho}(0)}{m^2_\rho}(s-m^2_\rho),$$
$$F^{\rm GS}_\pi(s)=\frac{m^2_\rho}{m^2_\rho-s-\tilde B_{\rho\rho}(s)}. \qquad (117)$$

Here $\tilde B_{\rho\rho}(s)$ is defined as our $B_{\rho\rho}(s)$ in (99) but omitting the $K\bar K$ contributions.

To compare the GS with our expression it is best to choose $F^+_\pi(s)$ (62) since no ω contributions are included in (117). Clearly, also the $K\bar K$ contributions are not included in (117), but one could easily do so replacing $\tilde B_{\rho\rho}(s)$ by the full $B_{\rho\rho}(s)$. The remaining difference between (117) and (62)– (64) is in the s-dependence of the effective ρ–γ coupling. The GS formula would correspond to the relation

$$\frac{1}{2}g_{\rho\to\pi\pi}\frac{f_\rho}{m_\rho}=1. \qquad (118)$$

Using the ρ^- parameters from our Fit III gives, however,

$$\frac{1}{2}g_{\rho\to\pi\pi}\frac{f_\rho}{m_\rho}=1.12\pm0.05. \qquad (119)$$

C Propagator matrix and form factors

In this appendix we give the derivation of the expressions (58), (59), and (62) for the form factors. We start with writing the inverse propagator matrix (53) as follows:

$$\Delta^{-1}_{\rm T}(s)=\left(\begin{array}{c|c}s&0\\\hline 0&\tilde\Delta^{-1}(s)\end{array}\right)+e\,s\left(\begin{array}{c|c}0&G^{\rm T}_{\gamma\to V}\\\hline G_{\gamma\to V}&0\end{array}\right), \qquad (120)$$

where

$$\tilde\Delta^{-1}(s)=\begin{pmatrix}-m^2_\rho+s+B_{\rho\rho}(s)&s\,b_{\rho\omega}+B_{\rho\omega}(s)\\ s\,b_{\rho\omega}+B_{\rho\omega}(s)&-m^2_\omega+s+B_{\omega\omega}(s)\end{pmatrix}$$

and

$$G_{\gamma\to V}=\begin{pmatrix}\frac{f_\rho}{m_\rho}+\frac{B_{\gamma\rho}}{e\,s}\\ \frac{f_\omega}{m_\omega}+\frac{B_{\gamma\omega}}{e\,s}\end{pmatrix}. \qquad (121)$$

The transverse propagator to order e then reads

$$\Delta_{\rm T}(s)=\left\{1+e\left(\begin{array}{c|c}0&G^{\rm T}_{\gamma\to V}\\\hline s\tilde\Delta(s)G_{\gamma\to V}&0\end{array}\right)\right\}^{-1}\left(\begin{array}{c|c}1/s&0\\\hline 0&\tilde\Delta(s)\end{array}\right)$$
$$=\left(\begin{array}{c|c}1/s&-eG^{\rm T}_{\gamma\to V}\tilde\Delta(s)\\\hline -e\tilde\Delta(s)G_{\gamma\to V}&\tilde\Delta(s)\end{array}\right)+O(e^2), \qquad (122)$$

$$\tilde\Delta(s)=(\det\tilde\Delta^{-1}(s))^{-1} \qquad (123)$$
$$\times\begin{pmatrix}-m^2_\omega+s+B_{\omega\omega}(s)&-s\,b_{\rho\omega}-B_{\rho\omega}(s)\\ -s\,b_{\rho\omega}-B_{\rho\omega}(s)&-m^2_\rho+s+B_{\rho\rho}(s)\end{pmatrix},$$

$$\det\tilde\Delta^{-1}(s)=(-m^2_\omega+s+B_{\omega\omega}(s))(-m^2_\rho+s+B_{\rho\rho}(s))$$
$$-(s\,b_{\rho\omega}+B_{\rho\omega}(s))^2. \qquad (124)$$

The pole masses and the pole widths of the ρ^0 and ω are obtained as solutions of

$$\det\Delta^{-1}_{\rm T}(s)=s\cdot\det\tilde\Delta^{-1}(s)=0. \qquad (125)$$

To obtain the expression for the electromagnetic form factor we use now (2), (57), (30), and (31). This gives with $q=p+p'$, $s=(p+p')^2=q^2$

$$\begin{aligned}&e(p'-p)_\mu F_\pi(q^2)\\&=\langle\pi^+(p')\pi^-(p)|J_\mu(0)|0\rangle\\&=\langle\pi^+(p')\pi^-(p)|A^\nu(0)|0\rangle\left(-g_{\mu\nu}q^2+q_\mu q_\nu\right)\\&=\langle\pi^+(p')\pi^-(p)||V^{(i)\lambda}(0)||0\rangle\\&\qquad\times\Delta^{(i,1)}_{\lambda\nu}(q)\left(-\delta^\nu{}_\mu q^2+q^\nu q_\mu\right)\\&=\langle\pi^+(p')\pi^-(p)||V^{(i)\lambda}(0)||0\rangle\Delta^{(i,1)}_{\rm T}(s)\left(g_{\lambda\mu}q^2-q_\lambda q_\mu\right)\\&=\langle\pi^+(p')\pi^-(p)||V^{(i)}_{{\rm T}\mu}(0)||0\rangle\,s\,\Delta^{(i,1)}_{\rm T}(s)\end{aligned} \qquad (126)$$

Inserting here (49), (50) and (122) leads to

$$F_\pi(s)=1-sG^{\rm T}_{V\to\pi\pi}\tilde\Delta(s)G_{\gamma\to V}, \qquad (127)$$

where

$$G_{V\to\pi\pi}=\begin{pmatrix}\frac{1}{2}g_{\rho\to\pi\pi}\\ \frac{1}{2}g_{\omega\to\pi\pi}\end{pmatrix}. \qquad (128)$$

We can further simplify the expression for F_π in (127) taking into account that $g_{\omega\to\pi\pi}$ is much smaller than $g_{\rho\to\pi\pi}$, and that the $\rho\omega$ mixing parameter is also small as becomes apparent from the fit. From (124) and (108) we get then

$$\det\tilde\Delta^{-1}(s)=(-m^2_\omega+s+B_{\omega\omega}(s))(-m^2_\rho+s+B_{\rho\rho}(s))$$
$$+O(g^2_{\omega\to\pi\pi},b^2_{\rho\omega},g_{\omega\to\pi\pi}b_{\rho\omega}). \qquad (129)$$

For $F_\pi(s)$ of (127) this gives

$$F_\pi(s)=1+\frac{1}{2}g_{\rho\to\pi\pi}\frac{\frac{f_\rho}{m_\rho}s+\frac{1}{e}B_{\gamma\rho}(s)}{m^2_\rho-s-B_{\rho\rho}(s)}$$

$$+\frac{1}{2}g_{\rho\to\pi\pi}\frac{\left(\frac{f_\omega}{m_\omega}s+\frac{1}{e}B_{\gamma\omega}(s)\right)(sb_{\rho\omega}+B_{\rho\omega}(s))}{\left(m_\rho^2-s-B_{\rho\rho}(s)\right)\left(m_\omega^2-s-B_{\omega\omega}(s)\right)}$$
$$+\frac{1}{2}g_{\omega\to\pi\pi}\frac{\frac{f_\omega}{m_\omega}s+\frac{1}{e}B_{\gamma\omega}(s)}{m_\omega^2-s-B_{\omega\omega}(s)}$$
$$+O(g^2_{\omega\to\pi\pi},b^2_{\rho\omega},g_{\omega\to\pi\pi}b_{\rho\omega}). \quad (130)$$

In a similar way we get for the $\gamma\pi$ transition form factor (14)

$$F_{\gamma\pi}(s)=F_{\gamma\pi}(0)-sG^{\mathrm{T}}_{V\to\pi\gamma}\tilde{\Delta}(s)G_{\gamma\to V}, \quad (131)$$

with $F_{\gamma\pi}(0)$ given by the anomaly (16) and

$$G_{V\to\pi\gamma}=\begin{pmatrix}\frac{g_{\rho\to\pi\gamma}}{m_\rho}\\ \frac{g_{\omega\to\pi\gamma}}{m_\omega}\end{pmatrix}. \quad (132)$$

Expanding in $g_{\omega\to\pi\pi}$ and $b_{\rho\omega}$ gives

$$F_{\gamma\pi}(s)=F_{\gamma\pi}(0)+\frac{g_{\rho\to\gamma\pi}}{m_\rho}\frac{\frac{f_\rho}{m_\rho}s+\frac{1}{e}B_{\gamma\rho}(s)}{m_\rho^2-s-B_{\rho\rho}(s)}$$
$$+\frac{g_{\omega\to\gamma\pi}}{m_\omega}\frac{\frac{f_\omega}{m_\omega}s+\frac{1}{e}B_{\gamma\omega}(s)}{m_\omega^2-s-B_{\omega\omega}(s)}$$
$$+\frac{sb_{\rho\omega}+B_{\rho\omega}(s)}{\left(m_\rho^2-s-B_{\rho\rho}(s)\right)\left(m_\omega^2-s-B_{\omega\omega}(s)\right)}$$
$$\times\left[\frac{g_{\rho\to\gamma\pi}}{m_\rho}\left(\frac{f_\omega}{m_\omega}s+\frac{1}{e}B_{\gamma\omega}(s)\right)\right.$$
$$\left.+\frac{g_{\omega\to\gamma\pi}}{m_\omega}\left(\frac{f_\rho}{m_\rho}s+\frac{1}{e}B_{\gamma\rho}(s)\right)\right]$$
$$+O(g^2_{\omega\to\pi\pi},b^2_{\rho\omega},g_{\omega\to\pi\pi}b_{\rho\omega}). \quad (133)$$

The weak form factor (13), F_π^+, is obtained from (130) setting $g_{\omega\to\pi\pi}=0$ and $b_{\rho\omega}=0$. This gives

$$F_\pi^+(s)=\frac{1}{m_\rho^2-s-B_{\rho\rho}(s)} \quad (134)$$
$$\times\left(m_\rho^2-s+\frac{1}{2}g_{\rho\to\pi\pi}\frac{f_\rho s}{m_\rho}-B_{\rho\rho}(s)+\frac{g_{\rho\to\pi\pi}}{2e}B_{\gamma\rho}(s)\right).$$

Using now (104) leads to (62).

References

1. J.J. Sakurai, Ann. Phys. **11**, 1 (1960); M. Gell-Mann, F. Zakhariasen, Phys. Rev. **124**, 953 (1961)
2. N.M. Kroll, T.D. Lee, B. Zumino, Phys. Rev. **157**, 1376 (1967)
3. G.J. Gounaris, J.J. Sakurai, Phys. Rev. Lett. **21**, 244 (1968)
4. J.H. Kühn, A. Santamaria, Z. Phys. C **48**, 445 (1990)
5. F. Klingl, N. Kaiser, W. Weise, Z. Phys. A **356**, 193 (1996)
6. M. Benayoun, H.B. O'Connell, A.G. Williams, Phys. Rev. D **59**, 074020 (2001)
7. J. Gasser, H. Leutwyler, Nucl. Phys. B **250**, 465 (1985); G. Ecker et al., Nucl. Phys. B **321**, 311 (1989)
8. G. Ecker et al., Phys. Lett. B **223**, 425 (1989); J.A. Oller, E. Oset, J.A. Palomar, Phys. Rev. D **63**, 114009 (2001)
9. A. Pich, J. Portoles, Phys. Rev. D **63**, 093005 (2001)
10. J.J. Sanz-Cillero, A. Pich, Eur. Phys. J. C **27**, 587 (2003)
11. Particle data group (C. Caso et al.), Eur. Phys. J. C **3**, 1 (1998); Particle data group (D.E. Groom et al.), Eur. Phys. J. C **15**, 1 (2000)
12. Particle data group (K. Hagiwara et al.), Phys. Rev. D **66**, 010001 (2002)
13. S. Anderson et al., Phys. Rev. D **61**, 112002 (2000)
14. R.R. Akhmetshin et al., Reanalysis of hadronic cross-section measurements at CMD-2, hep-ex/0308008
15. R.R. Akhmetshin et al., Phys. Lett. B **527**, 161 (2002)
16. M.N. Achasov et al., Phys. Lett. B **559**, 171 (2003)
17. A.V. Efremov, A.V. Radyushkin, Phys. Lett. B **94**, 245 (1980); S. Brodsky, G.P. Lepage, Phys. Lett. B **87**, 359 (1979)
18. V.V. Anisovich, D.I. Melikhov, V.A. Nikonov, Phys. Rev. D **52**, 5295 (1995)
19. V.V. Anisovich, D.I. Melikhov, V.A. Nikonov, Phys. Rev. D **55**, 2918 (1997)
20. D. Melikhov, Phys. Rev. D **53**, 2460 (1996); D. Melikhov, N. Nikitin, S. Simula, Phys. Rev. D **57**, 6814 (1998); D. Melikhov, B. Stech, Phys. Rev. D **62**, 014006 (2000); D. Melikhov, S. Simula, Phys. Rev. D **65**, 094043 (2002)
21. W. Kilian, O. Nachtmann, Eur. Phys. J. C **5**, 317 (1998)
22. S. Adler, Phys. Rev. **177**, 2426 (1969); J. Bell, R. Jackiw, Nuovo Cimento, A **60**, 47 (1969)
23. S. Brodsky, G.P. Lepage, Phys. Rev. D **24**, 1808 (1981)
24. O. Nachtmann, in Cargèse 1975, Proceedings, Weak and Electromagnetic Interactions At High Energies, Part A, edited by M. Levy et al. (Plenum Press, New York 1976)
25. S. Weinberg, Phys. Rev. D **6**, 1068 (1973)
26. L. Barkov et al., Nucl. Phys. B **256**, 365 (1985)
27. S.D. Protopopescu et al., Phys. Rev. D **7**, 1279 (1973); P. Estabrooks, A.D. Martin, Nucl. Phys. B **79**, 301 (1974)
28. R. Barate et al., Z. Phys. C **76**, 15 (1997)
29. C. Bebek et al., Phys. Rev. D **13**, 25 (1976); S. Amendolia et al., Nucl. Phys. B **277**, 168 (1986)
30. H. Goldstein, Classical mechanics, 2nd edition (Addison-Wesley, Massachusetts 1983)
31. S. Ghozzi, F. Jegerlehner, Isospin-violating effects in e^+e^- versus τ measurements of the pion form factor $|F_\pi(s)|^2$, hep-ph/0310181
32. J. Bijnens, G. Colangelo, P. Talavera, JHEP **05**, 014 (1998)
33. G. Parisi, R. Petronzio, Phys. Lett. B **94**, 51 (1980); V. Gribov, Eur. Phys. J. C **10**, 71 (1999); Yu. Dokshitzer, B. Webber, Phys. Lett. B **352**, 451 (1995); D.V. Shirkov, I.L. Solovtsov, Phys. Rev. Lett. **79**, 1209 (1997)